OPEN ACCESS Freely available online

PLoS GENETICS

A Role for Set1/MLL-Related Components in Epigenetic Regulation of the *Caenorhabditis elegans* Germ Line

Tengguo Li[1,2], William G. Kelly[1]*

1 Biology Department, Rollins Research Center, Emory University, Atlanta, Georgia, United States of America, **2** Graduate Program in Genetics and Molecular Biology, Emory University, Atlanta, Georgia, United States of America

Abstract

The methylation of lysine 4 of Histone H3 (H3K4me) is an important component of epigenetic regulation. H3K4 methylation is a consequence of transcriptional activity, but also has been shown to contribute to "epigenetic memory"; i.e., it can provide a heritable landmark of previous transcriptional activity that may help promote or maintain such activity in subsequent cell descendants or lineages. A number of multi-protein complexes that control the addition of H3K4me have been described in several organisms. These Set1/MLL or COMPASS complexes often share a common subset of conserved proteins, with other components potentially contributing to tissue-specific or developmental regulation of the methyltransferase activity. Here we show that the normal maintenance of H3K4 di- and tri-methylation in the germ line of *Caenorhabditis elegans* is dependent on homologs of the Set1/MLL complex components WDR-5.1 and RBBP-5. Different methylation states that are each dependent on *wdr-5.1* and *rbbp-5* require different methyltransferases. In addition, different subsets of conserved Set1/MLL-like complex components appear to be required for H3K4 methylation in germ cells and somatic lineages at different developmental stages. In adult germ cells, mutations in *wdr-5.1* or *rbbp-5* dramatically affect both germ line stem cell (GSC) population size and proper germ cell development. RNAi knockdown of RNA Polymerase II does not significantly affect the *wdr-5.1*–dependent maintenance of H3K4 methylation in either early embryos or adult GSCs, suggesting that the mechanism is not obligately coupled to transcription in these cells. A separate, *wdr-5.1*–independent mode of H3K4 methylation correlates more directly with transcription in the adult germ line and in embryos. Our results indicate that H3K4 methylation in the germline is regulated by a combination of Set1/MLL component-dependent and -independent modes of epigenetic establishment and maintenance.

Citation: Li T, Kelly WG (2011) A Role for Set1/MLL-Related Components in Epigenetic Regulation of the *Caenorhabditis elegans* Germ Line. PLoS Genet 7(3): e1001349. doi:10.1371/journal.pgen.1001349

Editor: Dirk Schübeler, Friedrich Miescher Institute for Biomedical Research, Switzerland

Received June 29, 2010; **Accepted** February 21, 2011; **Published** March 24, 2011

Funding: This work was supported by NIH GM63102 (WGK). The funders had no role in study design, data collection and analysis, decision to publish, or preparation of the manuscript.

Competing Interests: The authors have declared that no competing interests exist.

* E-mail: bkelly@biology.emory.edu

Introduction

The modulation of chromatin architecture is a key level of regulation for potentially all eukaryotic DNA-based processes including gene expression, and DNA replication, repair, and recombination [1]. One level of chromatin modulation involves the methylation of lysines in nucleosomal histones, which can be mono-, di-, or tri-methylated. The positions of methylated lysine residues, and even the extent of methylation at any single lysine, have been associated with distinct transcriptional outcomes [2]. For example, methylation at lysine 4 of histone H3 (H3K4me) correlates with transcriptional activation, whereas methylation on lysines 9 or 27 of H3 (H3K9me/H3K27me, respectively) is most often linked to gene repression [2,3]. Methyl groups are added to the lysine residues of histones by histone methyltransferases (HMTs) [4]. In *S. cerevisae*, the sole H3K4 HMT, Set1, is recruited to chromatin by the RNA polymerase II (Pol II) elongation machinery [5,6]. The occupancy of Set1 and H3K4 methylation are highly correlated on transcribing genes, with trimethylated H3K4 (H3K4me3) enriched in the 5′-end and dimethylated H3K4 (H3K4me2) extending further into the gene body [5,7,8]. Set1 is the only H3K4-specific HMT identified in *S. cerevisae*, yet it is not essential for yeast survival under laboratory growth conditions [9].

While some HMTs have detectable *in vitro* activity as isolated proteins, substantial and specific *in vitro* activities of the known H3K4-specific SET HMTs often require the addition of other components from their *in vivo* complexes [10–12]. The COMPASS complex, within which budding yeast Set1 operates, contains seven components that are important for Set1 activity (Table 1 and [13–16]). Components of the COMPASS complex are highly conserved from yeast to humans, although different subsets of the subunits are distributed among different H3K4 HMT complexes in multi-cellular organisms [10,17,18]. At least six Set1 homologs have been identified in mammalian cells: Set1A, Set1B, and four members of the Mixed-Lineage Leukemia (MLL) family: MLL1, −2, −3, and −4 [19–23]. The *S. cerevisiae* homologs of other components in the mammalian Set1/MLL complex(es) include RbBP5 (Swd1), WDR5 (Swd3), Ash2 (Bre2), Cfp1 (Spp1), and hDPY30 (Sdc1) (Table 1 and [19–22,24]). Biochemical studies suggest that WDR5/Swd3 and RbBP5/Swd1 are essential for complex stability and activity, whereas Ash2/Bre2 and Cfp1/Spp1 might play roles in the conversion from di- to tri-methylation [10,25,26]. Knockdown of WDR5 affects H3K4me1/2/3 to various degrees in mammalian cells [18], consistent with the idea that WDR5 plays a central role in stabilizing the complex and regulating its HMT activity [10,26].

Author Summary

The germ line transmits both genetic and epigenetic information between and across generations. The germ line uniquely retains developmental totipotency, and this property of germ cells is likely embedded in epigenetic information that is retained throughout the germ line cycle, within and across each generation. The methylation of Histone H3 on Lysine 4 (H3K4me) has been identified as both a mark of active transcription and a potential component of "epigenetic memory." We show that *C. elegans* homologs of components of a conserved H3K4 methyltransferase complex, the Set1/MLL complex, are important for normal H3K4 methylation in *C. elegans* germ cells and early embryos. Interestingly, Set1/MLL component dependent H3K4 methylation can occur independently of transcription in early embryonic germline and somatic blastomeres, and also in adult germline stem cells. A separate H3K4 methylation mechanism that operates independently of Set1/MLL component activities appears more dependent on ongoing transcription. We hypothesize that H3K4 methylation is maintained throughout the germ cell cycle by alternating transcription-dependent and -independent mechanisms that maintain this component of the germline epigenome.

Important developmental roles for this complex have been identified in multiple organisms. WDR5 is required for the maintenance of H3K4me3 levels at the HOXA9 and HOXC8 loci in mammalian cells and is important for the normal expression of these two genes [18]. In *X. laevis*, knockdown of WDR5 leads to reduction of H3K4me1 and H3K4me3 levels and a variety of developmental phenotypes including somatic and gut defects [18]. Previous studies in *C. elegans* have also implicated the Set/MLL complex as playing important roles in growth and somatic gonad and vulva development, at least partly through attenuation of Ras signaling [27,28].

Although some structural studies have suggested that WDR5 recognizes the most N-terminal residues of histone H3's "tail" [29–32], other studies have shown that H3 tail recognition by WDR5 may not require K4, as the interaction between WDR5 and the H3 tail can be independent of H3K4's methylation status.

Table 1. Conserved components of COMPASS complex in *C. elegans*.

S. cerevisiae	**Human**	*C. elegans*	*C. elegans**
set1	SET1 MLL1 MLL2 MLL3	C26E6.9 T12D8.1	*set-2* *set-16*
bre2	Ash2L	Y17G7B.2	*ash-2*
swd1	RbBP5	F21H12.1	*rbbp-5*
swd3	WDR5	C14B1.4 K04G11.4 ZC302.2	*wdr-5.1* *wdr-5.2* *wdr-5.3*
spp1	CxxC1/ Cfp-1	F52B11.1	*cfp-1*
swd2 *sdc1* *shg1*	WDR82 hDPY30	C33H5.6 ZK863.6 None	*wdr-82* *dpy-30*

* Nomenclature used in text and figures; modified from [28].

doi:10.1371/journal.pgen.1001349.t001

In contrast, asymmetric dimethylation of arginine 2 of H3 (H3R2me2a) abolishes binding of WDR5 to the H3 tail [33–35]. Recent studies indicate that MLL interacts with WDR5 through a WDR5-interacting (Win) motif that shares homology with the N-terminus of H3, and indeed the interaction site in WDR5 is the same for both MLL and H3 [36–40]. This suggests that interactions of WDR5 with H3 and MLL may be mutually exclusive. Intriguingly, *in vitro*-assembled complexes that lack the MLL protein still exhibit H3K4-specific HMT activity [38]. This suggests that MLL is not the sole HMT activity in the MLL complex, and that WDR5 binding to H3, to the exclusion of MLL, may not necessarily abrogate the complex's role in histone modification. In addition, histone demethylase activities are reported to copurify or otherwise interact with Set1/MLL core components, suggesting the complex may have a variety of roles in epigenetic regulation [27,41].

These studies have provided significant insight into how H3K4 methylation may be differentially regulated by components of the HMT complex, yet the contributions of this regulation to developmental pathways are still poorly understood. Indeed, the function of the H3K4me mark itself is unclear. Although H3K4 methylation has been assigned roles in the regulation of gene activation, it is also clearly a downstream consequence of gene activity. It has been proposed that H3K4 methylation could serve as a "memory" of where transcription has occurred, which in turn may stably guide further transcriptional regulation after cell division and throughout differentiation [42–44]. Recent data support this and suggest that histone methylation can serve as a component of epigenetic memory that can even be transferred intact across multiple generations. For example, mutation of the H3K4 demethylase LSD1/KDM1 causes an inappropriate and continued accumulation of H3K4me2 in germ cell chromatin across many generations [45]. This H3K4me2 accumulation correlates with a progressive, generation-dependent "germline mortality" phenotype in mutant populations, a phenotype that presumably results from the heritable accumulation of H3K4me2 that is not properly removed in the absence of LSD1 [45].

Another mark normally considered a product of ongoing transcription, H3K36me, has recently been shown by our lab and others to heritably mark, in embryos, genes that had last been expressed in the germ cells of the preceding generation [46]. This heritable marking is by a metazoan-specific H3K36 HMT, MES-4, that in *C. elegans* can operate in a largely transcription-independent mechanism. The role of MES-4 in this mode of "maintenance histone methylation" is essential for germline viability.

Recent studies in both mammals and worms have shown that histone modifications imposed in the paternal germ cells can be transferred into subsequent generations through sperm chromatin in mammals [47]. These include chromatin regions at genes transcribed in germ cells, but also so-called bivalent domains, regions marked by both H3K4 and H3K27 methylation, which have been observed to similarly mark inactive, developmental loci in ES cells [47–50]. Indeed, there is significant overlap in the loci marked by bivalent domains in both sperm and ES cells, suggesting that H3K4me can be maintained at these unexpressed loci in both germ cells and in embryonic lineages that retain pluripotency. Conversely in *C. elegans*, transcriptional inactivity of the X chromosome during male spermatogenesis results in the X chromosome being largely depleted of H3K4me during meiosis and gametogenesis; this dearth of H3K4me persists in spermatid chromatin, and is heritably maintained through multiple cell divisions in the early embryo [51].

Although epigenetic marks, including histone modifications and DNA methylation imprints, can be inherited from parents through

the gametes, there is significant erasure, or "reprogramming", of information in the zygote, and then again during germ cell specification [52–54]. The purpose of this reprogramming is unclear, but it is presumably related to the removal of epigenetic content that is incompatible with developmental pluripotency. Conversely, epigenetic information that defines the pluripotent state must be recognized and protected from erasure and/or actively maintained during this process. Many regions of the genome carrying this information may not be transcriptionally active during early embryonic stages, therefore maintenance of the epigenetic content may not be obligatorily coupled to transcriptional activity. Maintenance of transcription-associated marks like H3K4me and H3K36me may therefore require mechanisms operating outside of active gene expression. Evidence is mounting that such mechanisms exist. In addition to the maintenance of bivalent silenced loci and the MES-4 system mentioned above, a recent study in zebra fish embryos revealed a class of genes in which H3K4me3 alone is present at promoters with no evidence of ongoing transcription, further uncoupling this modification from transcription [55]. In addition, unmethylated CpG-rich regions of the genome can recruit H3K4 methylation independently of transcription, and this requires the Set1/MLL complex component Cfp1/CxxC1 [56]. These data indicate that H3K4 HMT complexes may play a role in the establishment and/or maintenance of H3K4me patterns in the genome independently of transcription.

RNA Polymerase II (Pol II) is normally inactivated in the early embryonic germline of *C. elegans* [57–59]. Despite the absence of Pol II activity, and cell divisions that could dilute this mark (through replication-coupled *de novo* chromatin assembly), the level of H3K4me2 in the germline precursor chromatin remains relatively stable [54]. This suggests the existence of transcription-independent mechanisms capable of maintaining this mark. In these studies, we show that conserved components of Set1/MLL-like histone methyltransferase complexes are required for what appears to be a largely Pol II-independent mode of H3K4me maintenance in germ cells. Interestingly, this mode predominates in early embryonic somatic and germline precursors, and in larval and adult stages Set1/MLL complex component-dependent H3K4 methylation is most obvious in the germline stem cell (GSC) population. Mutations in some components show defects in germline stem cell maintenance, impair fertility and germ cell development, and exhibit a germline mortality phenotype [28]. Our results suggest that H3K4 methylation is an important component of the epigenetic regulation of germline establishment, maintenance, and function. We propose that a combination of transcription-dependent insertion, and transcription-independent maintenance, of this mark may be required to maintain a totipotent epigenome as it passes through the germ line across generations.

Results

Conserved Set1/MLL complex components are present in the genome of *C. elegans*

H3K4me2 and me3 are considered to be hallmarks of transcriptional activity, as these marks are generally correlated with active genes in genome-wide studies [5,8,60,61]. However, significant levels of H3K4me2 are stably observed in the chromatin of early dividing blastomeres and germline precursors (P cells) of *C. elegans* embryos, which exhibit little detectable RNA Polymerase II transcription [57,59]. This suggests that transcription-independent mechanisms of maintaining this modification exist in these cells. We wished to identify the H3K4 methyltransferase(s) involved in the maintenance of this epigenetic mark and the consequences of their absence. All known H3K4 specific methyltransferases share the conserved catalytic SET-domain [62]. *C. elegans* contains 34 genes that encode SET domain proteins; sequence analysis suggests that two of them, *set-2* and *set-16*, are most closely related to yeast Set1 and human MLL H3K4 HMT's. The SET domain of worm *set-2* shares 80.6% and 74.2% homology with the human Set1A and yeast Set1 proteins, respectively, whereas the SET-domains of worm *set-16* and human MLL3 share 66.7% homology (not shown).

C. elegans also contains homologs of other yeast COMPASS components (see Table 1 for nomenclature). Because COMPASS is often used to refer to the specific complex found in *S. cerevesiae*, we hereafter refer to the *C. elegans* homologs of conserved components as Set1/MLL complex components to denote the metazoan complex. Note also that although homologs of most Set1/MLL complex components have been identified in *C. elegans*, the existence of a complex composed of these components can only be inferred at this time. Three homologues of *Swd3*/WDR5 (*wdr-5.1, wdr-5.2*, and *wdr-5.3*) are found in the *C. elegans* genome (Table 1 and [27,28]). Other homologues include: *F21H12.1* (*Swd1*/RbBP5), *Y17G7b.2* (*Bre2*/Ash2), *dpy-30* (*Sdc1*/hDPY30), *cfpl-1/F52B11.1* (*Spp1*/Cfp1), and *C33H5.6* (*Swd2*/Wdr82) (Table 1, and [27,28]). No *Shg1* homologs were identified in *C. elegans*. Previous studies have shown that a SET1/MLL complex, as in other organisms, contributes to H3K4 methylation in *C. elegans* [27,28]. Inactivation of the Set1 homolog *set-2* resulted in a global decrease of H4K4me3 levels in mixed-staged populations, but little detectable change in H3K4me2 levels [28]. Knockdown of each of three other worm homologs of the Set1/MLL complex components, *wdr-5.1*/WDR5, *dpy-30*/hDPY30, or *cfpl-1*/Spp1, resulted in decreases of both H3K4me2 and H3K4me3 to various degrees [28]. These experiments, while informative, did not assess stage- or tissue-specific effects of loss of these components, particularly in the germ line.

An essential role for Set1/MLL components in embryonic H3K4me regulation

To investigate how H3K4 methylation is regulated developmentally, we first asked if *set-2* or *set-16* was required for H3K4 methylation in early embryos. We dissected embryos from mutant strains and/or RNAi-treated animals and probed fixed whole mount specimens with antibodies specific to H3K4me2 or H3K4me3. In the RNAi protocol performed, treated animals are expected to exhibit reduction in both maternal and zygotic supplies of the targets. *set-16(RNAi)* caused >80% embryonic lethality, with survivors growing up to be Dumpy (*Dpy* phenotype) and sterile adults. In contrast, homozygous embryos from animals heterozygous for the *set-16 (gk438)* deletion allele (i.e., Maternal+/Zygotic-), developed into Dpy and sterile adults, indicating substantial maternal rescue. Appreciable loss of either di- or tri-methylated H3K4 (H3K4me2/me3) in any stage or tissue examined was not observed in either RNAi-treated or (maternally rescued) mutant embryos in our immunofluorescence assays (Figure S1 and data not shown). This result potentially differs from a recent report showing a decrease in H3K4me3 in *set-16* (RNAi) adults detected by western blot assays [27]; the differences in the respective results may be due to differences in the assays and experimental focus.

However, and similar to a previous report, we observed that H3K4me3 was substantially depleted from nuclei of *set-2 (tm1630)* deletion mutant embryos (Figure 1A; [28]). We also confirmed that H3K4me2 was not significantly affected in *set-2* mutant embryos (Figure 1B; [28]). Knockdown of *set-2* by RNAi caused similar reduction in H3K4me3 levels in embryos, also without

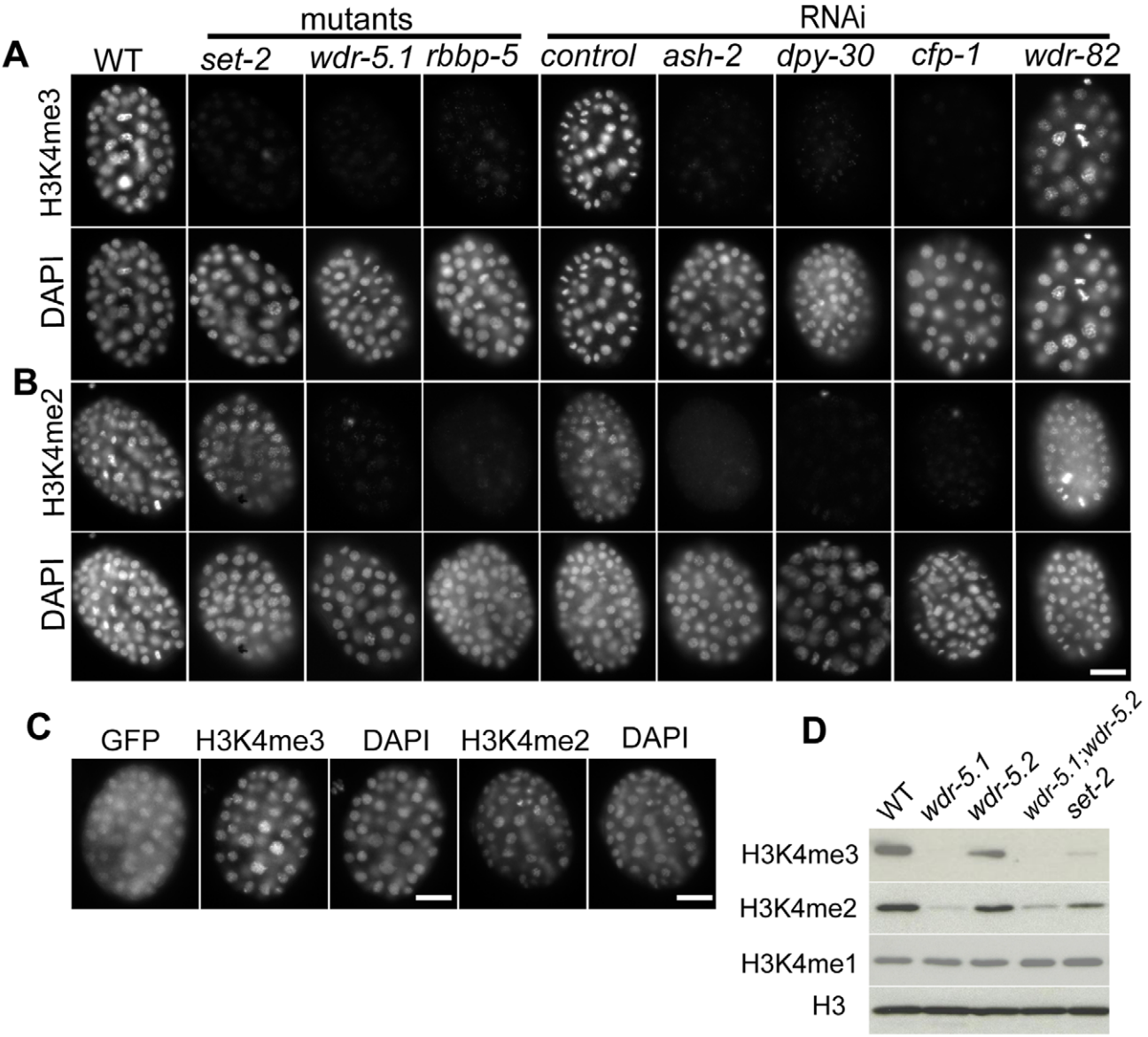

Figure 1. Set1/MLL complex components are largely responsible for H3K4me2/3 in embryos. Embryos were dissected from WT, mutant, or RNAi treated adult *eri-1*(*mg366;* enhanced RNAi) animals. RNAi mediated knockdown was used for *ash-2, dpy-30, cfp-1 and wdr-82*. Embryos were probed with rabbit anti-H3K4me3 (Panels in A) or mouse anti-H3K4me2 monoclonal antibodies (Panels in B); DNA was counter-stained with DAPI. Exposure times were the same for each condition. Scale bars represent 10um. (A and B) H3K4me3 and H3K4me2 are present in chromatin of wild-type embryos, but both are dramatically decreased in chromatin of embryos from *wdr-5.1* and *rbbp-5* mutants, and embryos from *ash2, dpy-30, or cfp-1* RNAi treated mothers. H3K4me3, but not H3K4me2, is reduced in *set-2(tm1630)* mutant embryos. RNAi mediated knockdown of *wdr-82* did not affect either H3K4me3 or H3K4me2. (C) A *wdr-5.1::GFP* transgene rescues H3K4 methylation in the *wdr-5.1(ok1417)* mutant. *wdr-5.1(ok1417);wdr-5.1::GFP* transgenic embryos were probed with antibodies against GFP and H3K4me3/2 as indicated. H3K4me3/2 were restored in the chromatin of early embryos in which WDR-5.1:GFP expression was detected. (D) Western blot of lysates from mixed stage *wdr-5.1(ok1417), wdr-5.2(ok1444), wdr-5.1;wdr-5.2* double mutant, and *set-1(tm1630)* mutant embryos. The blots were probed with anti-histone H3, anti-H3K4me1, mouse monoclonal anti-H3K4me2 or rabbit polyclonal anti-H3K4me3 antibodies, as indicated. H3K4me3/2 levels were dramatically decreased in strains with the *wdr-5.1(ok1417)* allele, whereas H3K4me3 levels were more strongly depleted than H3K4me2 in *set-2(tm1630)*. H3K4me1 levels were not noticeably affected in any mutant strain tested.
doi:10.1371/journal.pgen.1001349.g001

affecting H3K4me2 (data not shown). These results indicate that SET-2 is an HMT principally responsible for H3K4me3, and that other HMTs may regulate H3K4me2. We do not know if SET-2 acts to convert H3K4me2 to H3K4me3, but we did not notice any increase in H3K4me2 levels in *set-2* mutants, as might be expected from a defect in such conversion (not shown).

In an attempt to identify the additional HMT(s) responsible for H3K4me2, we knocked down several additional SET domain containing H3K4 HMT candidates including: *F15E6.1 (set-9)*, *Y51H4a.2 (set-26)*, *K09F5.5 (set-12)*, *Y41D4b.12 (set-23)*, *lin-59*, *set-25*, and *F25D7.3* by RNAi. We did not detect changes in H3K4me2/3 by immunofluorescence in any of these experiments (data not shown). These results confirm and extend the findings of others that SET-2 is the HMT activity that is largely responsible for H3K4 trimethylation in embryos ([28]). The dimethyl H3K4 HMT activity still remains to be identified.

To test whether the other conserved components of Set1/MLL complexes are similarly required for normal H3K4me regulation in embryos, we examined animals with mutations in the homologous genes and/or treated with RNAi targeting those loci. We first focused on the WDR5 homologs. Similar to *set-2(tm1630)* mutant embryos, H3K4me3 was strongly depleted from the nuclei of *wdr-5.1(ok1417)* embryos (Figure 1A). The *wdr-5.1(ok1417)* deletion allele is likely a null allele since an antibody against WDR-5.1 did not detect the WDR-5.1 band in western blot analyses (Figure S2), and *wdr-5.1(RNAi)* resulted in phenotypes similar to *ok1417* (not shown). However, unlike *set-2(tm1630)*, significant loss of H3K4me2 was also observed in *wdr-5.1* embryos, albeit not to the near background levels observed for H3K4me3 (Figure 1B). These defects are specific to loss of WDR-5.1 activity in the deletion mutants since both H3K4me2 and H3K4me3 defects could be rescued by a WDR-5.1::GFP transgene (Figure 1C). In contrast, neither mutation of *wdr-5.2*, nor knockdown of *wdr-5.3* by RNAi, the other Swd3/WDR5 homologs, noticeably affected H3K4me3 or H3K4me2 levels in embryos, nor did combinations with *wdr-5.1(ok1417)* mutants exhibit additive defects in H3K4me (data not shown). These data indicate that among the WDR5 homologs, WDR-5.1 plays the predominant role in H3K4 methylation in early embryonic stages. Protein blot analysis of H3K4me2 and H3K4me3 marks present in embryos confirmed the immunofluorescence results (Figure 1D). H3K4me1 levels were not detectably affected in any of the mutants tested (Figure 1D and data not shown).

We then examined other conserved Set1/MLL components. As with *wdr-5.1(ok1417)* mutants, both H3K4me3 and H3K4me2 were strongly reduced in the nuclei of *rbbp-5(tm3463)* mutant embryos (Figure 1A and 1B). Knockdown of *rbbp-5* by RNAi resulted in similar defects, indicating our RNAi experimental conditions were efficient (data not shown). We then targeted homologs of other Set1/MLL complex components in an RNAi hyper-sensitive strain, *eri-1(mg366)*. As shown in Figure 1A and 1B, *ash-2*, *dpy-30*, and *cfp-1* are also required for normal levels of both H3K4me3 and H3K4me2 in early embryos. RNAi of *wdr-82* showed no discernible effects on H3K4 methylation in our assays. Interestingly, H3K4 methylation was observed to become increasingly detectable in later stages of embryogenesis (>300 cells) in mutant and RNAi-treated embryos (Figure S3 and data not shown). This indicates that HMT activities independent of these components exist in the embryo, and that the H3K4 marks provided by these activities become increasingly evident as development progresses.

Taken together, these data show that conserved homologs of Set1/MLL components contribute to the predominant mode of H3K4me regulation in early *C. elegans* development. All of the predicted complex components, with the exception of *wdr82/swd-2*, are essential for this HMT activity. SET-2 appears to be the H3K4 HMT operating in the context of this putative complex that is specifically required for H3K4 trimethylation, whereas a separate as yet unidentified HMT activity is responsible for H3K4me2 regulation. In later embryos, H3K4 methylation becomes detectable in the absence of Set1/MLL component function; this H3K4 methylation activity may correlate with a transcription-dependent process (see below).

WDR-5.1 binding to H3 is dependent on H3R2 methylation

As mentioned, WDR5 is thought to play a central role in core complex assembly and HMT regulation by interacting with MLL and/or histone H3 N-terminal tails [10,18]. Binding of WDR5 to the histone H3 N-terminus is not affected by lysine 4 methylation, but instead is strongly inhibited by asymmetric dimethylation of arginine 2 (H3R2me2a) [33,34]. To test if worm WDR-5.1, like its mammalian WDR5 counterpart, has similar interactions with the H3 tail, we incubated wild-type nuclear extract with biotinylated H3 peptides and assayed for WDR-5.1 interactions by western blot analysis of peptide-bound material using a WDR-5.1 specific antibody. As shown in Figure S4, WDR-5.1 showed specific interactions with unmodified (H3K4me0) and H3K4me2 peptides, but not with an H3R2me2a-modified peptide. *C. elegans* WDR-5.1 thus has similar histone H3 binding characteristics to those of mammalian WDR5. These data, in addition to the H3K4 methylation defects observed in *wdr-5.1*, *rbbp-5*, and *ash-2(RNAi)* animals described above, strongly suggest that the these proteins probably exist in a complex that has similar attributes to other bona fide Set1/MLL complexes.

Set1/MLL-dependent H3K4 methylation maintenance in the early embryo is largely independent of transcription

The COMPASS complex is recruited to chromatin by the RNA polymerase II (RNA Pol II) holoenzyme complex in *S. cerevisiae* [5], and thus in yeast H3K4 methylation appears to be strictly dependent on transcriptional elongation. However, as discussed earlier, there is growing evidence that H3K4 methylation in metazoans may not always be coupled to ongoing transcription.

In *C. elegans* embryonic germline precursors (P cells) there is little or no Pol II transcription [58] yet H3K4 methylation persists through the four cell divisions in this lineage. However, some differences are observed between di- and tri-methylated forms (Figure 2 and [54]). In wild type embryos, H3K4me3 is present from P1 and P2, but is decreased by 30% and by ~85% in P4, respectively (Figure 2C and 2F), whereas H3K4me2 is maintained at comparable levels in P1 through P4 (Figure 2E). The levels of both H3K4me2/3 are essentially uniform in all somatic blastomere chromatin in all early stages. In *wdr-5.1/wdr-5* mutant embryos both H3K4me2 and H3K4me3 are initially observed in the chromatin of 1-2 cell nuclei; this is presumably inherited from the gamete chromatin, as it is also strongly retained in the polar bodies (Figure 2B, 2D; arrowheads) [51]. However, the maintenance of both marks in subsequent cell divisions is severely compromised in the P cells of *wdr-5.1* embryos (Figure 2B, 2D). The loss is presumably through replication-coupled histone replacement, or other types of histone dynamics, as the levels decrease with cell number. Notably, H3K4me2/3 in the somatic cells were also strongly reduced in the absence of *wdr-5.1* (Figure 1, Figure 2). Similar results were observed in the *rbbp-5/swd-1* mutant, as well after RNAi of *ash-2*, *dpy-30*, and *cfp-1* (data not shown). These data suggest that Set1/MLL component- dependent mechanisms are responsible for maintaining normal levels of H3K4me2/3 in the transcriptionally inactive P cells and early somatic blastomeres. Early development is largely driven, and cell viability largely maintained by maternal supplies in *C. elegans*, so the early somatic blastomeres are not thought to be robustly active [63]. The maintenance of H3K4me2/3 in these early somatic lineages may thus also be largely independent of ongoing transcription

To further investigate this discordance between Set1/MLL mediated H3K4 methylation and active transcription, we knocked down *ama-1* (the large, catalytic subunit of RNA Pol II) by RNAi in both WT and *wdr-5.1* mutants. Under the conditions employed, *ama-1(RNAi)* resulted in 100% embryonic lethality and AMA-1 protein dropped to undetectable levels by immunofluorescence in early embryos (Figure 3). In addition, the RNAi conditions employed were sufficient to abolish detection of the phospho-Ser2 modification on RNA Pol II (Ser2p; recognized by the H5 monoclonal antibody), which correlates with the elongating form

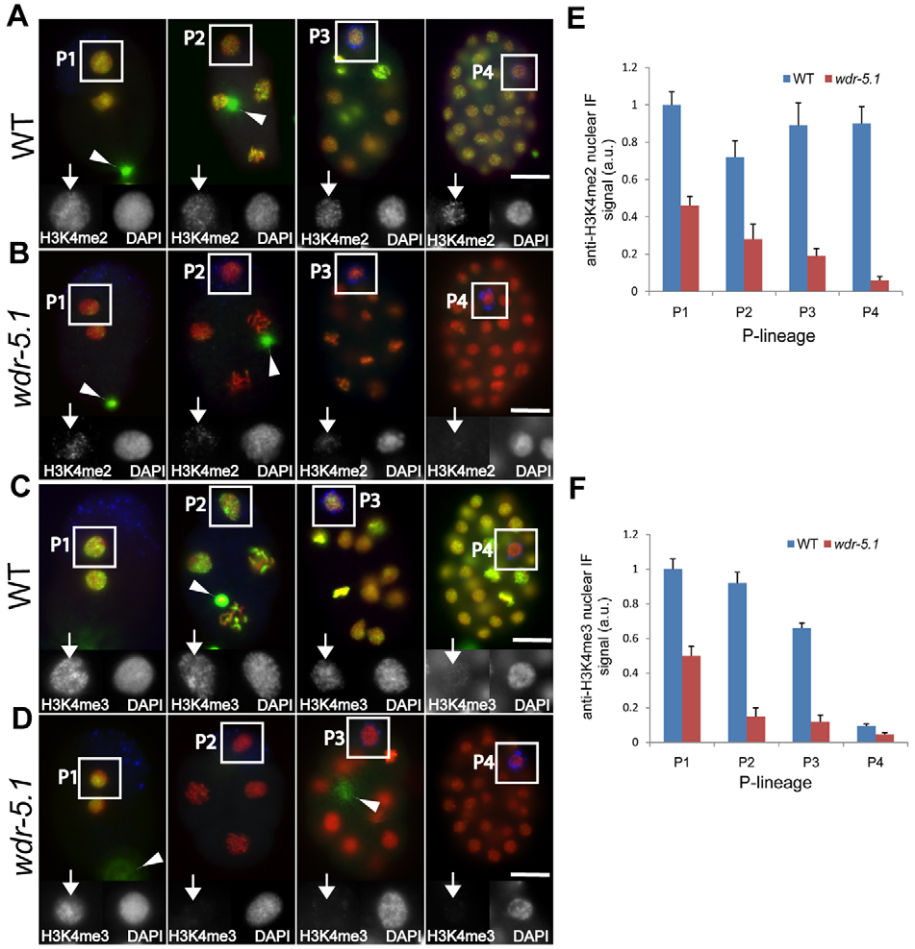

Figure 2. WDR-5.1 is required for H3K4 methylation in embryonic cells that lack RNA Pol II activity. Embryos from wild-type and *wdr-5.1(ok1417)* animals were probed with mouse monoclonal antibody to H3K4me2 (A, B) or rabbit polyclonal antibody to H3K4me3 (C,D) in green, and anti-PGL-1 or mouse monoclonal antibody OIC1D4 to mark the germline precursors, P1–P4 (blue), and counterstained with DAPI (red). P-blastomeres are boxed and enlarged grayscale images are shown in insets with arrows marking chromatin stained for H3K4me2/3 as indicated. Arrowheads mark out-of-focus polar bodies, which retain oocyte chromatin and associated modifications. Images were taken of each sample with identical exposure times for each respective probe for comparison. mRNA production does not occur in wild-type germline P-blastomeres, yet H3K4me2 levels remain relatively constant in P1–P4 in these nuclei (A). H3K4me3, in contrast, has significantly declined by P4 (C). All H3K4me2 and H3K4me3 methylation in both the P-blastomeres and early somatic blastomeres is dependent on WDR-5.1 function (B,D). Bar = 10um. (E and F) Quantification of anti-H3K4me2/me3 signals in the P cell nuclei. The mean anti-H3K4me2/3 IF intensity in each nucleus was normalized to the mean DAPI fluorescence intensity. Normalized signals were compared to the normalized mean of wild type P1 nuclei, which was arbitrarily set to 1. For each P-cell stage (P1–P4), 3–5 nuclei in similar states of chromatin condensation were measured in each experiment. The graph represents results from 3 independent experiments. a.u. = arbitrary units. Error bars = SEM.
doi:10.1371/journal.pgen.1001349.g002

of the RNA Pol II holoenzyme (Figure S5A). The depletion of AMA-1 in wild-type embryos did not significantly impact H3K4me3/me2 levels, and this *ama-1(RNAi)* "resistant" H3K4 methylation was not observed when *wdr-5.1* was also defective (Figure 3). RNAi of *cdk-9*, the kinase component of the essential RNA Pol II transcription elongation factor pTEF-b, also knocked down Pol II Ser2p to undetectable levels and this also had no appreciable effect on H3K4me3/2 maintenance (Figure S5). We could not test if the WDR-5.1-independent H3K4 methylation we observed in later stages was also depleted by either RNAi, since the embryos arrested prior to those stages (not shown). Taken together with what we observed in the P cells above, these data strongly suggest that in all early embryonic nuclei, including germline precursors, H3K4 methylation maintenance is largely Set1/MLL component-dependent, and this activity is unaffected by significant reduction of ongoing transcription.

H3K4 methylation in adult germ cells has a unique mode of regulation

We next asked whether the Set1/MLL components are similarly required for H3K4me regulation in post-embryonic tissues. A recent report has shown that a worm MLL-like complex can attenuate Ras signaling in vulva development, but the vulva defects are only observed in a sensitized genetic background [27]. In our hands, mutants in some of the Set1/MLL component homologs, such as *wdr-5.1/wdr-5* and *rbbp-5/swd-1*, exhibited fertility defects (below), so we focused on the adult germ line. In *C. elegans*, hermaphrodite germ cells first undergo spermatogenesis in larvae followed by a switch to oogenesis, which is maintained in adults. The adult germ cells are linearly and progressively arranged by developmental stage within the gonad arms, such that defects in any particular stage are easily identified. The mitotically active germ line stem cells (GSCs) reside in the most

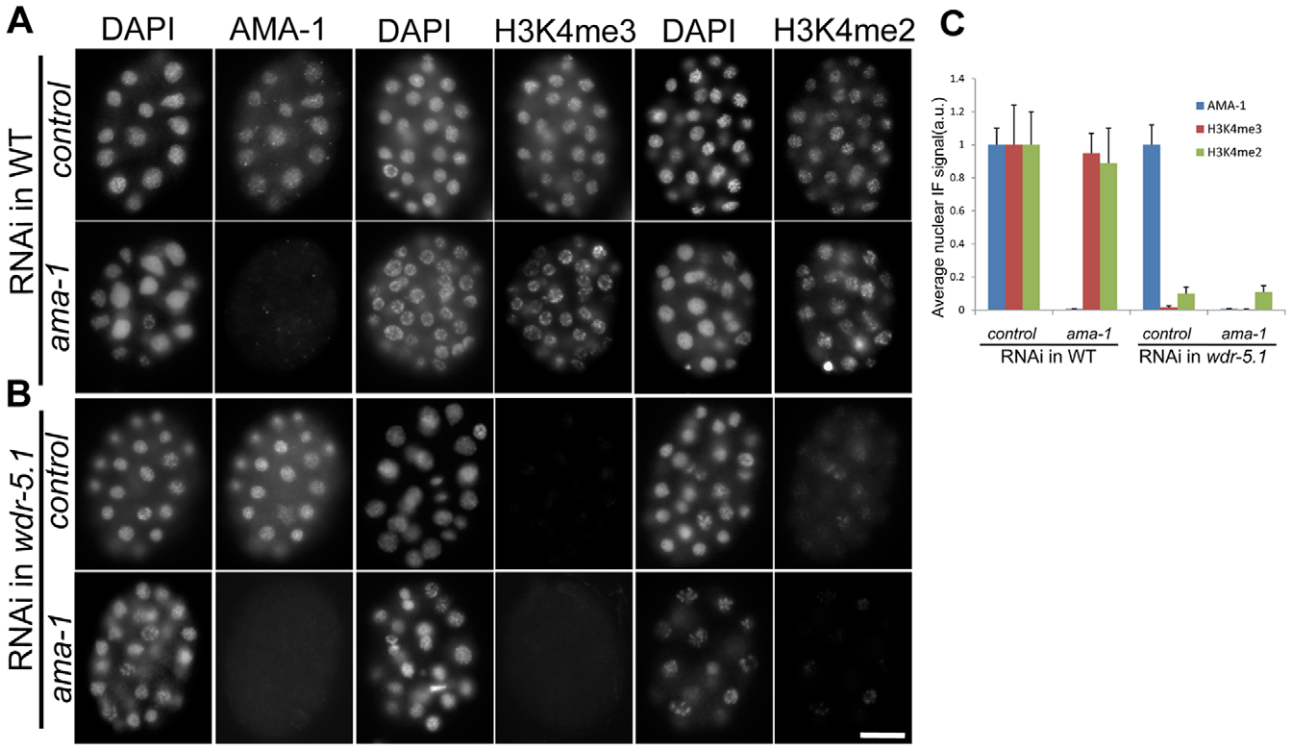

Figure 3. RNAi knock-down of *ama-1* does not affect WDR-5.1–dependent H3K4 methylation in early embryos. L4 larvae of WT and *wdr-5.1* animals were soaked in dsRNA targeting the large subunit of RNA Pol II (encoded by *ama-1*), or 1x soaking buffer in control samples (as described in Materials and Methods), and their embryos were fixed and probed with either 8WG16 (AMA-1 protein) or mouse monoclonal antibodies against H3K4me2/3 as indicated. For each antibody immunofluorescence, exposure times were determined by the unsaturated exposure of an interphase nucleus of control WT embryos, this time was used for sample comparisons within each experimental set. (A) Substantial AMA-1 depletion was achieved in *ama-1(RNAi)* embryos, but H3K4me2/3 were not substantially affected. (B) The H3K4 methylation resistant to *ama-1(RNAi)* is depleted in *wdr-5.1(ok1417)* embryos. Bar = 10um. (C) Quantification of anti-AMA-1, H3K4me2 or H3K4me3 relative immunofluorescence in embryonic chromatin. Individual interphase nuclei were chosen and the mean IF signal intensity of anti-H3K4me3 or H3K4me2 at a mid-nucleus focal plane was measured. 5 nuclei from each of 3 embryos at similar stages were measured and analyzed as in Figure 2. Anti-AMA-1, H3K4me3 and H3K4me2 signals (arbitrary units ± SEM) were normalized to DAPI. Normalized signals were compared to those of RNAi controls, which were arbitrarily set to 1. The graph represents results from 2 independent experiments.
doi:10.1371/journal.pgen.1001349.g003

distal region of the gonads, and their entry into and progression through meiosis and gametogenesis occur sequentially as the cells move more proximally (e.g., left to right in Figure 4). The border between mitotic exit and meiotic entry, for example, is readily visualized by a characteristic condensation and crescent-shaped localization of all chromosomes within each nucleus in the "transition zone", comprising leptotene and zygotene stages. After exiting the transition zone, germ cells progress proximally into pachytene and then further on into oogenesis. H3K4me3 and H3K4me2 are normally abundant in the chromatin of all adult germ cell stages, and both are broadly distributed on all autosomes (Figure 4A and Figure 5A). These marks, however, are generally absent from the X chromosomes in all germ cell stages, with the exception of oogenesis [51,64].

We first examined the role of the Set1/MLL component homologs in H3K4me3 regulation in adult germ cells. H3K4me3 was dramatically decreased in a specific population of nuclei in *set-2(tm1630)*, *wdr-5.1(ok1417)* and *rbbp-5(tm3463)* deletion mutants. The decrease we observed was limited to chromatin in the most distal nuclei, the region within which the germline stem cell population (GSC) resides (Figure 4). This pattern was identical to that observed with RNAi knockdown of *set-2*, *wdr-5.1*, or *rbbp-5*, indicating that these cells are not specifically resistant to RNAi (not shown). Interestingly, and in contrast to what we observed in embryos, RNAi mediated knockdown of *ash-2*, *dpy-30* or *cfp-1* had minimal effects on H3K4me3 levels in adult germ cell chromatin compared to the near 90% reduction observed in *set-2*, *wdr-5.1* and *rbbp-5* mutants (Figure 4). Consistent with our results in embryos, *wdr-82* knockdown also did not affect H3K4me3 in adult cells (data not shown). Significant H3K4me3 loss was also restricted to the GSCs in *wdr-5.1* males, showing that the requirement for *wdr-5.1* and *rbbp-5* for GSC H3K4me3 is not sex-specific (Figure S6A).

The absence of redundancy and the highly overlapping H3K4me3 defect patterns in these three mutants are evidence that SET-2, WDR-5.1 and RBBP-5 work together in these cells. The absence of H3K4me defects observed with RNAi of *ash-2*, *cfp-1*, or *dpy-30* indicates that, unlike in embryonic cells, these conserved components are not required for H3K4 methylation in the adult germline stem cells. The GSCs are not less susceptible to RNAi gene targeting, since RNAi of *set-2*, *wdr-5.1*, or *rbbp-5* substantially knocks down methylation of H3K4 in the GSCs and *ama-1(RNAi)* was effective in this region of the gonad. Furthermore, RNAi mediated knockdown of *ash-2*, *cfp-1*, and *dpy-30* all significantly affected H3K4 methylation in offspring from treated animals, and the lack of effect in the adult germ cells was observed in both the parents and similarly exposed adult siblings of affected embryos in these experiments (details diagrammed in Figure S7).

As the germ cells in the *set-2*, *wdr-5.1*, and *rbbp-5* mutants progressed into meiosis, increasing levels of H3K4me3 was detected in the chromatin of pachytene stage and more proximal

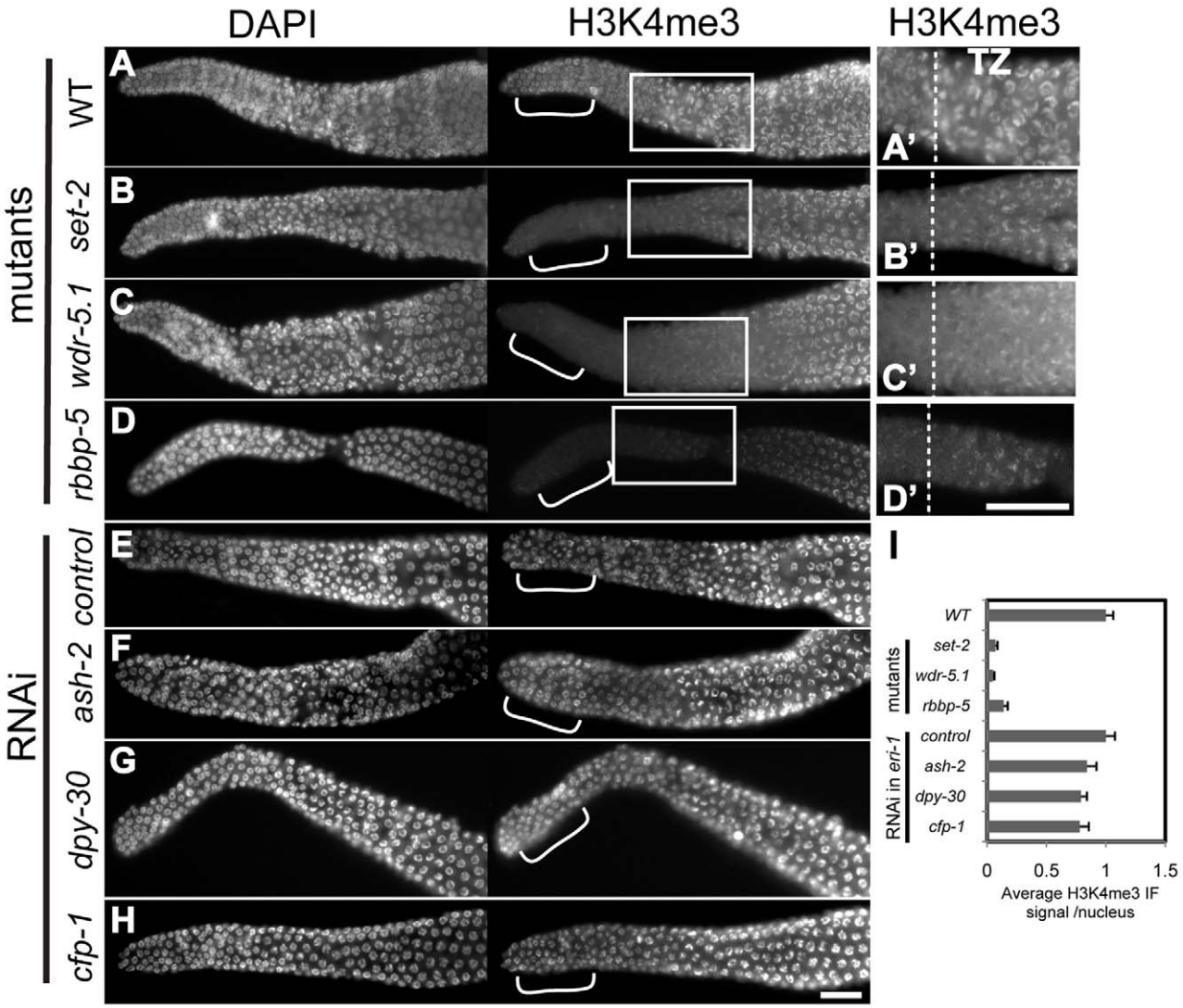

Figure 4. H3K4me3 in adult GSCs is regulated by a subset of Set1/MLL complex components. Dissected and fixed whole-mount adult gonads were probed with rabbit H3K4me3 antibodies and counter-stained with DAPI. Exposure times were the same for each condition. Gonads are displayed with the distal regions to the left; dashed lines in magnified views in A'–D' indicate where transition zone (transition from mitosis to meiosis) begins in each gonad. Images were taken with identical exposures for each probe and at the same magnification for comparison. Brackets highlight the region where nuclei were chosen for quantification (I). Scale bars represent 20um. (A–D) Wild-type (WT; N2) or indicated mutant strains; (E–H) *eri-1(mg366)* animals treated with control RNAi or RNAi targeting the indicated genes. H3K4me3 is present in the chromatin of all germ cell stages in wild-type animals, but is substantially decreased in nuclei of the distal mitotic germline stem cells (GSCs) in *set-2(tm1630), wdr-5.1(ok1417), and rbbp-5(tm3463)* mutants. In contrast, RNAi knockdown of *ash-2, dpy-30,* or *cfp-1* in *eri-1(mg366)* did not significantly affect H3K4me3 levels. (I) Quantification of anti-H3K4me3 signals in distal nuclei. The mean IF intensities of individual nuclei were measured using Simple PCI software. 20–25 nuclei were measured from 3–5 gonads (4–5 nuclei/gonad) H3K4me3 signals (arbitrary units ± SEM) were normalized to mean DAPI intensity. Normalized signals were compared to those of wild type or RNAi controls, which were arbitrarily set to 1. The graph represents results from 2 independent experiments.
doi:10.1371/journal.pgen.1001349.g004

nuclei (Figure 4A'-4D'). However, the levels of H3K4me3 in pachytene and diakinesis regions in *wdr-5.1* were significantly reduced compared to wild type levels (Figure S8A–S8C). The *wdr-5.1/rbbp-5*-independent mechanism in meiotic germ cells may be additive to, or partially dependent on, what is placed in the chromatin by the WDR-5.1–dependent processes in the GSCs. Indeed it is also possible, and we cannot rule out by these experiments, that the separate mechanisms have separate targets. Transcription in adult germ cells appears to be highest in meiosis [65], so the *wdr-5.1* independent H3K4 methylation may be similar to the Set1/MLL-independent H3K4 methylation observed in late-stage embryos (Figure S3). These results indicate that the regulation of H3K4me3 in embryos and adult GSCs depends on an HMT activity that requires different subsets of the "panel" of Set1/MLL components. The results also indicate that an additional, Set1/MLL component independent mode of H3K4 trimethylation is predominantly active in meiosis.

We also tested for H3K4me2 changes in mutant and/or RNAi-treated adult germ cells. We found that, like H3K4me3, H3K4me2 in the GSC region was also only slightly affected by knockdown of *ash-2*, *dpy-30*, or *cfp-1* (Figure 5E–5F). As in embryos, *set-2*, which is required for H3K4me3 maintenance, also was dispensable for H3K4me2 in adult germ cells (Figure 5B). Similar to H3K4me3, H3K4me2 levels were decreased 90% and

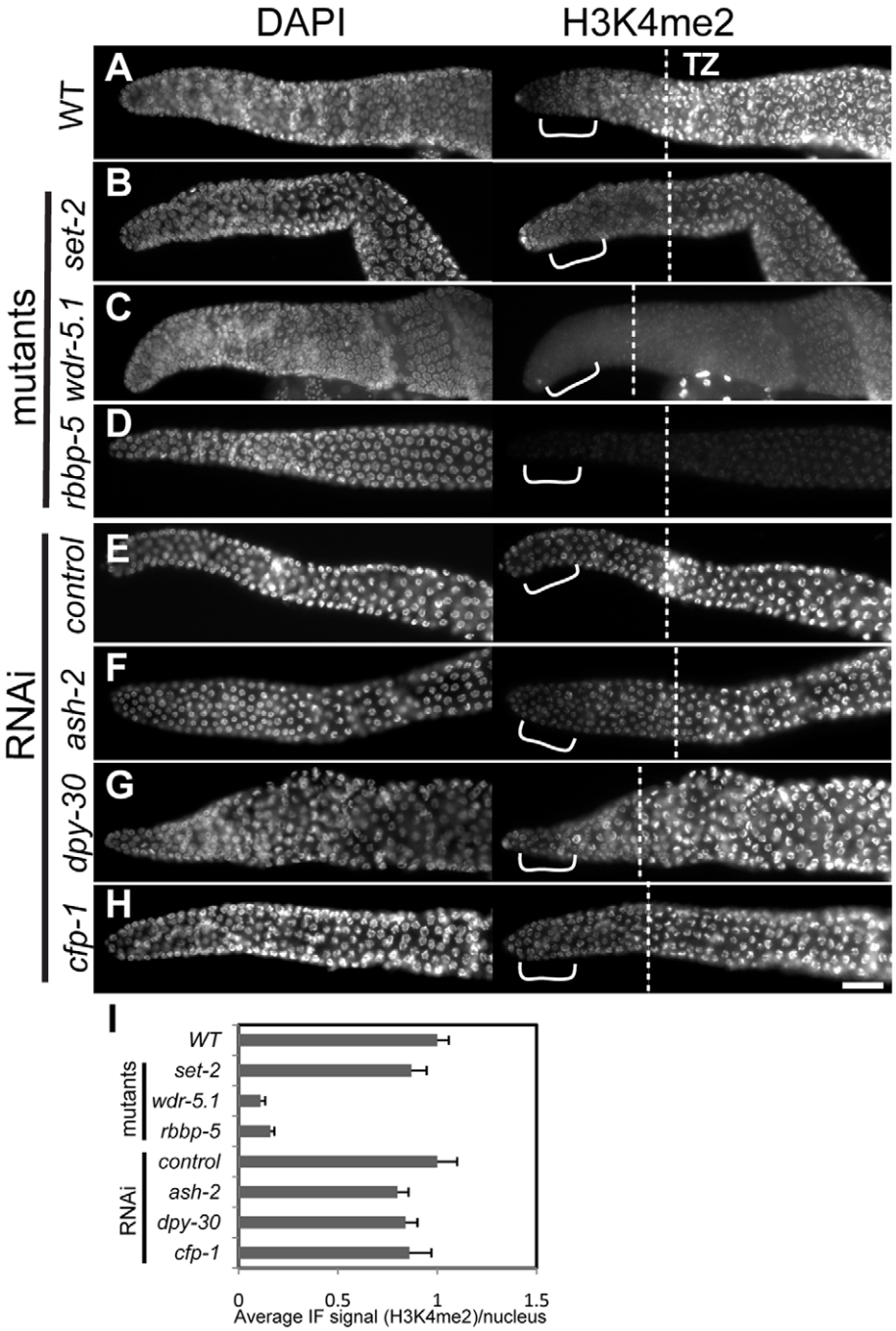

Figure 5. H3K4me2 in adult GSCs is also regulated by a subset of Set1/MLL complex components. Experiments and data presented as in Figure 4. Samples were probed with mouse monoclonal antibody (CMA303) against H3K4me2. H3K4me2 is substantially reduced in the chromatin of distal GSCs in *swd-3(ok1417)* and *rbbp-5(tm3463)* mutants (A-D), but appears unaffected in either *set-2(tm1630)* mutants, or *eri-1(mg366)* animals treated with RNAi as indicated (E-H). Bars represent 20 um. (I) Quantification of anti-H3K4me2 signals in distal nuclei. The quantification of nuclei in region marked by brackets was done as in Figure 4. H3K4me2 signals (arbitrary units ± SEM) were normalized to wild-type germ cell nuclei. The graph represents results from 2 independent experiments.
doi:10.1371/journal.pgen.1001349.g005

85% in the GSC region of *wdr-5.1(ok1417)* and *rbbp-5(tm3463)* mutant gonads, respectively (Figure 5I). RNAi of these two genes again showed similar defects in adult germ cells (data not shown). However, as shown in Figure S9, H3K4me2 was reduced but not completely absent in the distal region of *wdr-5.1(ok1417)* gonads. Low levels of H3K4me2 are apparent, with longer exposure times, as discreet foci on the chromosomes, rather than the more diffuse chromatin pattern observed in wild-type GSC nuclei (Figure S9C). As with H3K4me3, H3K4me2 appeared in pachytene and diakinesis regions, and was also 50% below that of WT chromatin (Figure S9A and S9D). These defects and patterns were also observed in *wdr-5.1* males (Figure S6B).

Notably, we observed similar defects in H3K4me2 staining (in both adults and embryos) in the *wdr-5.1* strain using two different

monoclonal antibodies from mouse [66] and rabbit (Millipore cat# 04-790). A significant decrease was also observed using a polyclonal antibody, but to a lesser extent (Millipore cat#, 07-030). Both the mouse monoclonal and polyclonal antibody signals were efficiently reduced when competed with H3K4me2 peptides, but not with H3K4me0, H3K4me1, or H3K4me3 peptides (not shown). The reason for the increased residual signal detected by the polyclonal antibody in the mutants is not known.

These results show that WDR-5.1 and RBBP-5 are essential for normal H3K4me2 and H3K4me3 in adult GSCs, and to a lesser extent, meiotic germ cells and (as in embryos) appear to rely on different HMT activities for the differently methylated products. Furthermore, some Set1/MLL components that are essential for H3K4 methylation in embryos do not appear to be required in adult germ cells. Regulation of H3K4 methylation in *C. elegans,* as in mammals, may therefore involve distinct HMT complexes to yield a variety of different outcomes in different tissues and developmental stages. There also appears to be H3K4-specific HMT activities in *C. elegans* that can be roughly divided into those that share a requirement for at least some homologs of the Set1/MLL components, and those that do not. The H3K4 methylation activities we observe in meiotic chromatin and in later embryonic stages appear to fall into the latter class.

H3K4me maintenance by WDR-5.1/RBBP-5–dependent mechanisms in adult GSCs is largely independent of ongoing transcription

As described earlier, H3K4me2/3 maintenance in the embryonic blastomeres and germline precursors was not appreciably affected by the significant disruption of RNA Pol II activity. We investigated whether this was also the case in adult germ cells by targeting *ama-1* with RNAi. AMA-1 protein is detectable in all adult germ cell chromatin until diakinesis stage in oogenesis, which largely lack RNA Pol II associated with chromatin (Figure 6A-a' and c'; data not shown and [67]). In both *ama-1(RNAi)* and *wdr-5.1;ama-1(RNAi)* animals, AMA-1 protein was depleted to undetected levels in the distal GSCs and in the more distal early- to mid-pachytene meiotic nuclei, but was still faintly detectable in more proximal nuclei (Figure 6A-b' and d'). This is consistent with the more proximal (older) nuclei containing AMA-1 protein that had been translated prior to mRNA depletion by RNAi treatment. These results indicate that the RNAi had efficiently knocked down AMA-1 to undetected levels in distal- to mid-proximal germ cells in both genotypes in these experiments. Furthermore, the progression of germ cell development appeared to be crippled in these animals, as oocyte production had ceased, and 100% of all embryos produced up to the time point of analysis failed to hatch (not shown).

In parallel experiments, H3K4me3 and H3K4me2 patterns in *ama-1(RNAi)* gonads showed an interesting defect. In wild-type gonads treated with *ama-1* RNAi, H3K4me2/3 levels in the GSCs (where H3K4me is dependent on *wdr-5.1*) were not significantly affected (Figure 6). However, a swath of nuclei that had recently entered into and engaged in meiosis showed a 60–70% decrease in the levels of H3K4me3 and H3K4me2 (Figure 6B-b', f', brackets; and 6C and 6D, red bars). Note that both the GSCs and this "swath" of distal meiotic nuclei showed comparable depletion of AMA-1 protein in parallel animals, but H3K4me levels were only decreased in the meiotic nuclei (Figure 6A-b' and d'). Late pachytene nuclei that exhibited AMA-1 antibody staining in parallel animals still showed significant H3K4me2/3 levels (Figure 6C, green bars). In *wdr-5.1;ama-1(RNAi)* animals, H3K4me2/3 was dramatically decreased in all nuclei from the distal GSC region to the mid-meiotic nuclei; i.e., the *ama-1(RNAi)* resistant H3K4 methylation in the GSC region was not observed (Figure 6B; d',h', 6C and 6D). We also analyzed *ama-1(RNAi)* wild-type and *wdr-5.1(ok1417)* animals using the H5 (Pol II phospho-Ser2) antibody, and confirmed that the elongating form of RNA Pol II was depleted in the treated germ cells (Figure S10A and S10B). H3K4me3 in GSC chromatin was again largely unaffected in wild-type *ama-1* (RNAi), whereas that in meiotic chromatin was significantly depleted (Figure S10C). *In wdr-5.1; ama-1(RNAi)* germ cells, both GSC and meiotic cell again showed reduced H3K4me3 in these experiments (Figure S10D).

Taken together, our data suggest that the H3K4 methylation in GSCs, that is largely dependent on *wdr-5.1/rbbp-5* mediated mechanisms, is also largely impervious to substantial depletion of RNA Pol II. We cannot conclude that all Pol II activity was completely eliminated in these experiments, but the lack of anti-AMA-1 and anti-Pol II phospho-Ser2 signals, and the fully penetrant embryonic lethality preceding the cessation of oogenesis, indicates substantial ablation of ongoing transcription in the treated germ cells. Importantly, a significant component of H3K4 methylation that occurs in meiotic cells is largely independent of WDR-5.1, and this methylation was dramatically affected by the *ama-1(RNAi)* conditions employed. The meiosis-coupled H3K4 HMT activity is thus more closely linked to ongoing transcription. Thus WDR-5.1/RBBP-5-dependent mechanisms can maintain H3K4 methylation in both the embryonic germline and their post-embryonic germline stem cell descendants in a largely RNA Pol II independent manner. We next investigated the role of WDR-5.1 in the larval transitions that bridge these germ cell stages.

Transitional regulation of H3K4me3/2 in proliferating larval germ cells

The H3K4 methylation that is maintained by Set1/MLL components in the transcriptionally inert P-blastomere chromatin is dramatically erased in the primordial germ cells (PGCs), named Z2 and Z3 [54]. The reduction in H3K4me is maintained throughout embryogenesis, and normally does not reappear until hatching (Figure 7A and [54]). The re-appearance of H3K4me2/3 at hatching usually coincides with reappearance of the phospho-Ser2 modification of RNA Pol II, and thus presumably the re-initiation of productive transcription in these cells [68]. PGC proliferation in early stage larvae produces the germline stem cells that ultimately contribute to and maintain the adult germ cell population. In wild-type animals, H3K4me2/3 are present at robust levels in all germ cell nuclei at all post-embryonic stages. In *wdr-5.1(ok1417)* mutants, H3K4me3 reappearance was initially normal in the early PGCs and their progeny in L1 larvae, and remained detectable for a few cell divisions (Figure 7B). However, as the number of germ cells increased, H3K4me3 levels substantially decreased in the proliferating (now established) GSCs in *wdr-5.1* L2 and early L3 larvae.

In later larval stages, as the *wdr-5.1(ok1417)* germ cells began to enter meiosis, H3K4me3 was observed to again accumulate in their chromatin, as observed in *wdr-5.1* adult gonads (e.g., Figure 4). The H3K4me2 pattern was similarly defective in *wdr-5.1* mutants (data not shown). These results indicate that concomitant with PGC reactivation, there is a period of *wdr-5.1*-independent H3K4 methylation as the GSCs first become established. Shortly thereafter, and during all subsequent larval and adult stages, H3K4 methylation in the proliferating GSCs becomes largely dependent on the WDR-5.1 mechanism.

WDR-5.1 and RBBP-5 are required for normal GSC maintenance

The GSCs are the proliferative cells that support the large numbers of gametes ultimately produced by *C. elegans* adults.

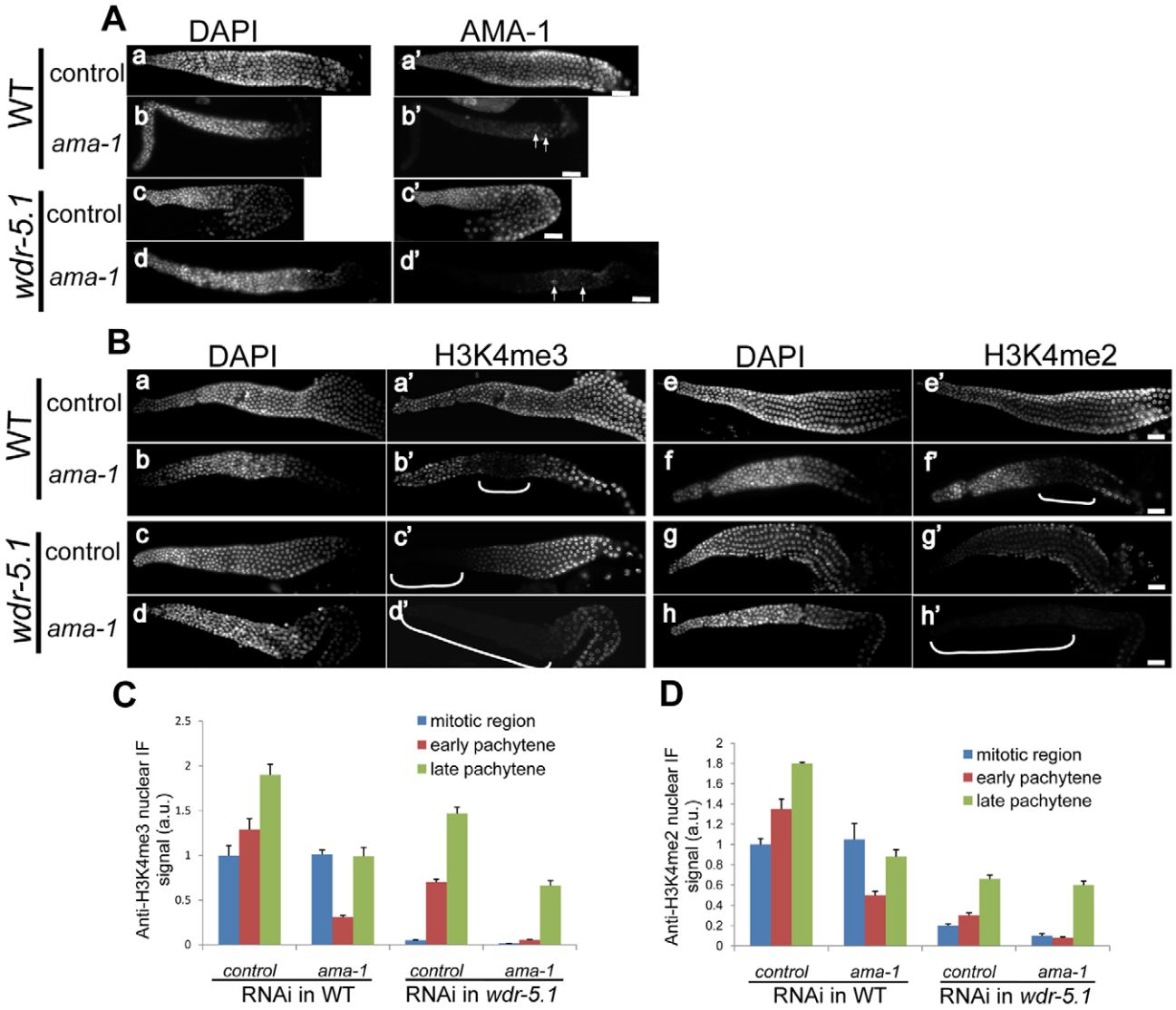

Figure 6. WDR-5.1–dependent H3K4 methylation in adult GSCs is unaffected by depletion of *ama-1*. Wild-type (A) and *wdr-5.1(ok1417)* (B) animals were treated with control RNAi or *ama-1(RNAi)*. The gonads from treated animals were dissected, fixed, and probed with anti-AMA-1(8WG16), or mouse monoclonal antibody against H3K4me2/3 as indicated. Exposure times were the same for each antibody for comparison. (A) AMA-1 is undetectable in the RNAi treated gonads from both WT and *wdr-5.1(ok1417)* animals except in more proximally-located (older) nuclei (arrows) (b′ and d′). (B) In gonads from parallel *ama-1(RNAi)* treated wild-type animals, a broad band of nuclei that lacks both H3K4me3 and H3K4me2 is apparent from the transition/meiotic entry zone to the region where AMA-1 protein is still detectable (b′, f′ brackets). The band excludes the distal GSCs. In *wdr-5.1(ok1417); ama-1(RNAi)* gonads, all distal nuclei lack H3K4me2/3, including the GSCs (highlighted by brackets in B; d′ and h′). Scale bars represent 20um. (C and D) Quantification of anti-H3K4me2 or H3K4me3 signals in the germ cell nuclei from different regions of the gonad. Nuclei were randomly chosen from distal proliferative region, early pachytene (marked by brackets in b′ and f′) and late pachytene regions. Signals were measured and quantified as in Figure 4. For each stage, 12 nuclei from 3 gonads were quantified. Anti-H3K4me3 and H3K4me2 signals (arbitrary units ± SEM) were normalized to distal nuclei from RNAi controls. The graph represents results from 2 independent experiments.
doi:10.1371/journal.pgen.1001349.g006

Mutations that affect the maintenance of this stem cell population affect the number of nuclei and thus the length of the pre-meiotic region of the gonad arms [69-71]. We examined the effect of *wdr-5.1* and *rbbp-5* mutations on the length of the GSC zone in young adult gonads. The established procedure is to measure the number of cell diameters from the most distal nucleus (the distal tip cell) to the first nuclei exhibiting the crescent-shaped chromosome morphology characteristic of cells entering early prophase I of meiosis (“transition zone” nuclei; e.g.; [70]). We also assayed for SYP-1 appearance, a synaptonemal complex protein [72], to help identify the boundaries between the mitotic region and transition zone (Figure 8B, 8D and 8F).

A temperature-dependent defect was observed for GSC maintenance in both *wdr-5.1* and *rbbp-5* mutants: at 25°C the mutants exhibited shorter GSC zones (average 11 cell diameters) compared to identically staged wild-type animals (average 18 cell diameters; Figure 8G). Indeed, some *wdr-5.1* animals had GSC zones as short as 6 cell diameters (Figure 8G). The brood size of *wdr-5.1* mutants was also substantially lower than wild-type animals, even at normal temperatures (Figure S11A). These data suggest that the H3K4me2/3 marks in the GSC chromatin that are maintained by the WDR-5.1/RBBP-5 dependent mechanisms, or the proteins themselves, may be important for normal maintenance of this stem cell population.

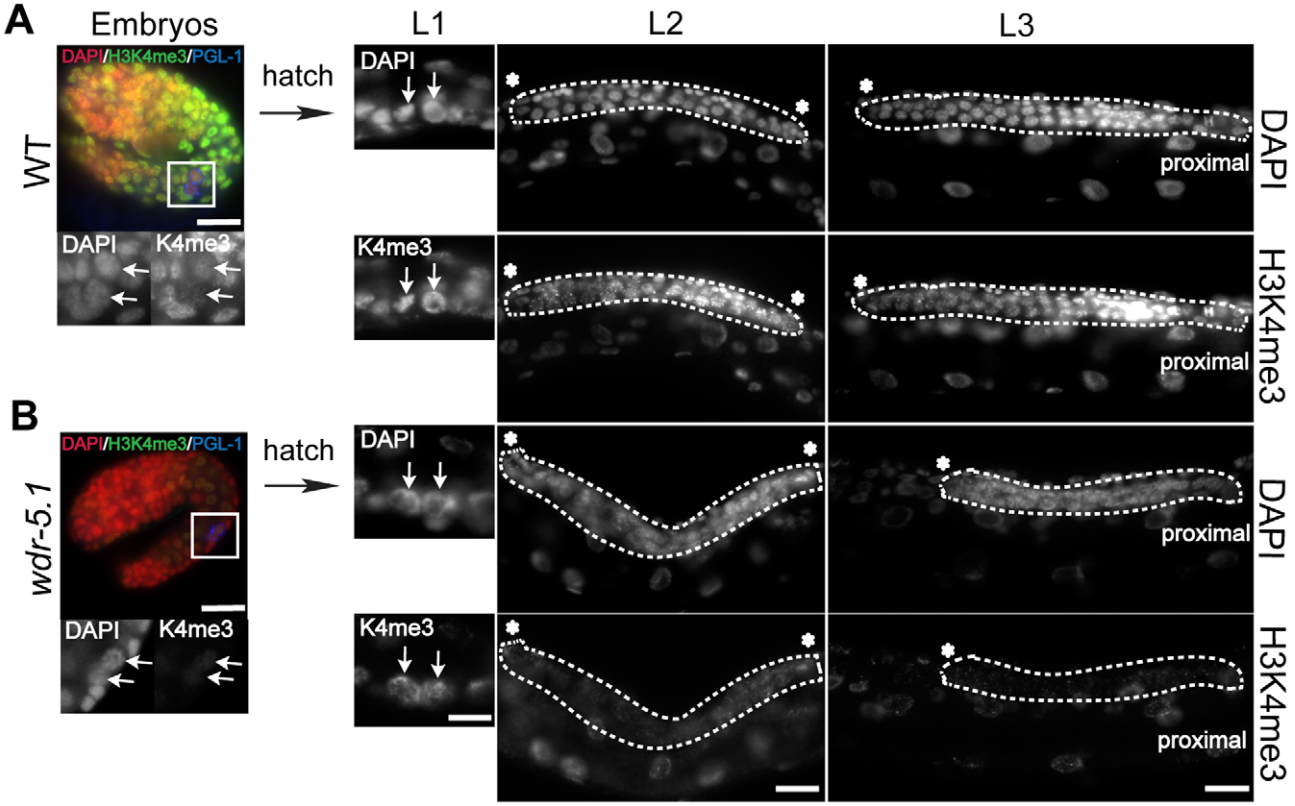

Figure 7. H3K4me3 is transiently independent of WDR-5.1 activity in early proliferating larval germ cells. Two-fold stage embryos and larvae at L1, L2, and L3 stages were probed for H3K4me3 and PGL-1 (to identify the germ cells), and counterstained with DAPI. Arrows and dashed lines highlight germ cells in embryos and larval gonads. The primordial germ cells (PGCs, marked by PGL-1 staining in blue), Z2 and Z3 (arrows), are boxed and enlarged in the embryo images. Red: DAPI; Green: H3K4me3; Blue: PGL-1. In the larval stage images, the full gonad is outlined at the indicated stages except in L3 larvae, in which just one gonad arm is illustrated and outlined. H3K4me3 is absent from PGC chromatin ([54] and A; embryos), but reappears after hatching in both WT (A; L1, arrows) and *wdr-5.1* (B; L1, arrows) larvae. In WT larvae, H3K4me3 persists through all larval germ cell stages (A; L1, L2, L3). H3K4me3 is initially present in *wdr-5.1* L1 germ cell chromatin (B; L1), but is greatly reduced in later larval germ cells (B; L2 and L3). Thus only the initial appearance of H3K4me3 in post-embryonic germ cells is not dependent on WDR-5.1 function. Asterisks indicate distal end of gonad arms. Bars = 10 um.
doi:10.1371/journal.pgen.1001349.g007

wdr-5.1 and *rbbp-5* mutants display only partially overlapping somatic and germline developmental phenotypes

We further characterized the phenotypes of *set-2*, *wdr-5.1* and *rbbp-5* mutants. *set-2(tm1630)* mutants do not display obvious phenotypes when grown at either 20°C or 25°C (Table 2), indicating that neither SET-2 or its H3K4me3 mark are overtly essential for normal development. At 20°C, *wdr-5.1* animals were fertile, but showed 12% embryo lethality (Emb) and a moderate egg laying defect (Egl) (Table 2 and Figure S12A). In contrast, at 20°C, *rbbp-5(tm3465)* mutants exhibited multiple phenotypes including a Dumpy phenotype (Dpy), egg-laying defect (Egl), and significant sterility (24.4%; Table 2 and Figure S12A and S12B). The Dpy phenotype was not observed in *wdr-5.1(ok1417)* animals at any temperature, indicating that these factors may have non-overlapping roles in some somatic developmental pathways. The basis of the Dpy phenotype in *rbbp-5(tm3465)* animals, for which many candidate pathways exist, is unknown.

At elevated temperatures, *wdr-5.1(ok1417)* embryonic lethality rose dramatically to 29% for the 1st generation at 25°C, and a previously reported germline mortality phenotype in subsequent generations was also confirmed (Figure S11B and [28]). When grown at 25°C, the mutant exhibited an increased frequency of sterile progeny with each generation. By the F4 generation, 67% of the embryos developed into sterile adults. Interestingly, sterility reached a maximum by the F4 generation, although the number of offspring produced by the few fertile animals at subsequent generations was low (Figure S11B and not shown). When *rbbp-5* L4 larvae were shifted to 25°C, 12.1% of their F1 progeny arrested as embryos; however, most (82.9%) of the survivors developed into sterile adults (Table 2). The remainder appeared to be capable of producing sperm and oocytes, since some embryos were observed in these animals *in utero*, yet these embryos were not laid onto the plates nor did they hatch (Table 2).

In vertebrates, mutations in WDR5 and MLL cause developmental defects, presumably because of their reported roles in regulation of Hox gene expression [18,73]. Because of the embryonic lethality we observed in *wdr-5.1* and *rbbp-5* mutants, we tested for defects in Hox gene expression. We examined the expression of the Hox loci *lin-39*, *ceh-13*, *mab-5 and egl-5* in *wdr-5.1* mutant embryos grown at 20°C by qRT-PCR. We found no significant alteration in the expression levels of these four genes in *wdr-5.1(ok1417)* compared to wild type embryos, suggesting that WDR-5.1 is not required for Hox gene expression at normal temperatures in *C. elegans* (data not shown).

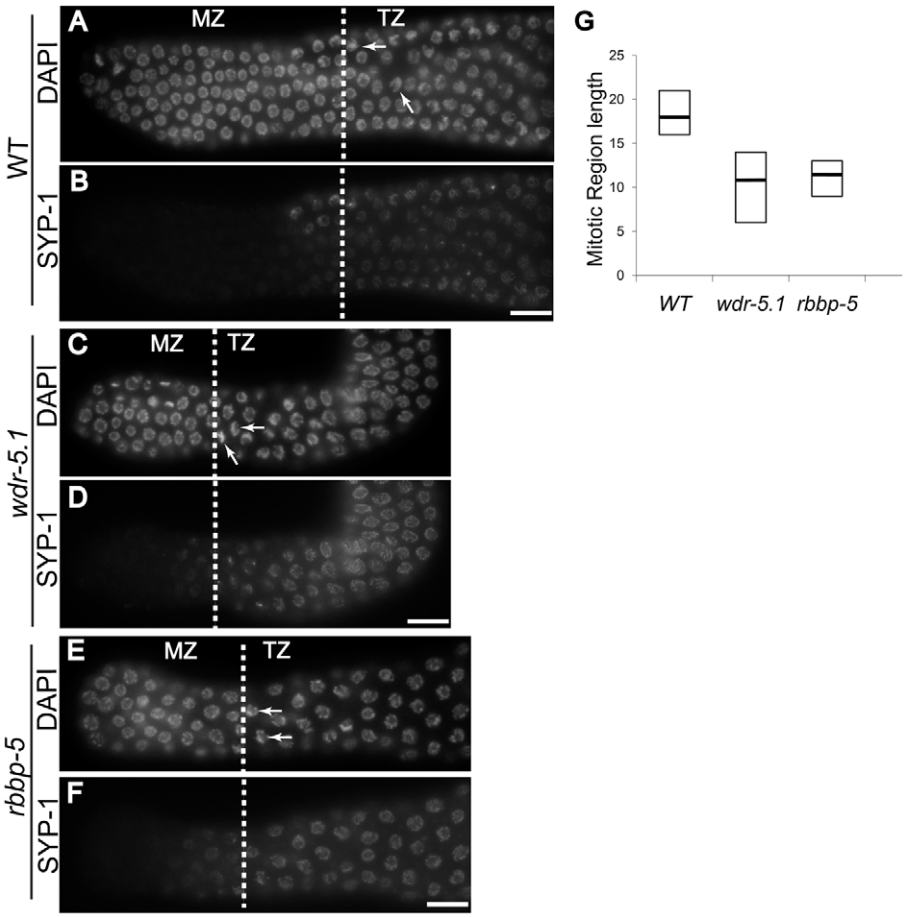

Figure 8. ***wdr-5.1 and rbbp-5*** **mutants exhibit temperature-sensitive GSC defects.** L4 larvae were picked and shifted to 25°C for 24 hours. Gonads were dissected, fixed and probed with antibodies for SYP-1 protein, and counter stained with DAPI. The length of the germline stem cell compartment in each gonad was determined by counting the number of mitotic zone (MZ) nuclei from the distal tip to the beginning of the transition zone (TZ) of each gonad (dashed lines). The MZ/TZ boundary was identified by characteristic nuclear morphology and appearance of the synaptonemal complex protein, SYP-1. (A–F) SYP-1 and DAPI stained gonads from wild-type (WT), *wdr-5.1(ok1417)*, and *rbbp-5(tm3463)* adult hermaphrodites; dashed lines indicate boundary between MZ and TZ. Arrows mark the crescent morphology of nuclei in TZ. Scale bars = 10 um. (G) Box-plot showing distribution of MZ lengths observed from strains in (A); black line indicates median; top and bottom indicates maximum and minimum lengths observed for each strain. The number of gonads examined for each strain (n) is as follows: WT = 32, *wdr-5.1(ok1417)* = 43, *rbbp-5(tm3463)* = 25.
doi:10.1371/journal.pgen.1001349.g008

wdr-5.1/WDR5 and *RBBP-5/RbBP5* mutants exhibit defects in germ cell development

To investigate the mechanism underlying the sterility of *wdr-5.1(ok1417)* and *rbbp-5(tm3463)* mutants, we dissected the gonads from sterile worms and stained with DAPI. We found that 75.9% of the gonads in sterile *wdr-5.1(ok1417)* mutants grown at 25°C had endomitotic oocytes (Emo phenotype); i.e., unfertilized eggs had prematurely entered the cell cycle and engaged multiple rounds of replication in the absence of cytokinesis (Figure 9B and 9D; Class I). In addition, a small percentage of hermaphrodite gonads (5.1%) exhibited a Mog (masculinization of germline) phenotype in which only sperm were produced; i.e., the normal switch from

Table 2. Phenotypic analysis of the HMTase core complex component mutants.

	Embryo Lethality		Sterility	
	20°C	**25°C**	**20°C**	**25°C**
WT	0.6% (n = 619)	2.7% (n = 1509)	0 (n = 114)	0.75% (n = 133)
set-2 (tm1630)	0.5% (n = 871)	11.5% (n = 893)	0.8% (n = 114)	1.9% (n = 104)
wdr-5.1 (ok1417)	12% (n = 1201)	36% (n = 557)	2.5% (n = 119)	29% (n = 89)
rbbp-5 (e1834)	3.18% (n = 345)	12.1% (n = 173)	24.4% (n = 104)	82.9% (n = 88)*

* 82.9% had no embryos; 17.1% exhibited dead embryos *in utero*.
doi:10.1371/journal.pgen.1001349.t002

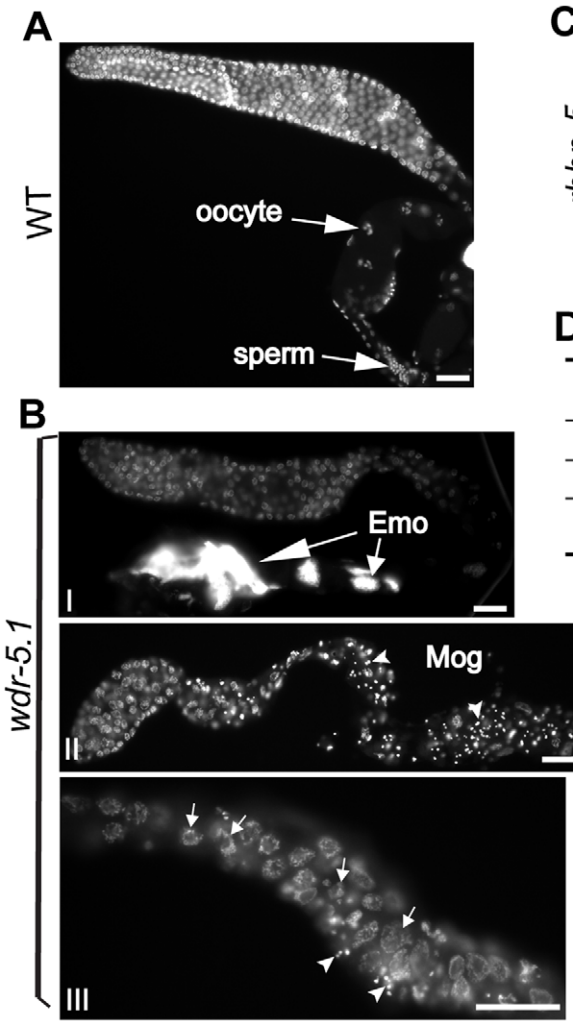

	wdr-5.1 (n=116)	*rbbp-5* (n=73)
Class I (Emo)	75.9%	100%
Class II (Mog)	5.1%	0
Class III (Nuclear Morphology)	19.0%	0

Figure 9. Temperature-sensitive germ cell development defects in *wdr-5.1* and *rbbp-5* mutants. L4 larvae were shifted to 25°C overnight, whole-mount fixed and stained with DAPI. (A) Wild-type hermaphrodite gonad showing normal germ cell development at 25°C from distal mitotic (upper left), and meiotic stages leading to proximal oocytes and sperm in spermatheca (lower right). (B) Examples and classification of defects observed in *wdr-5.1(ok1417)* 25°C mutants. Class I: Emo = endomitotic oocytes (oocytes that prematurely activate and undergo DNA endoreduplication); Class II: Mog = masculinization of germ line (fail to switch from spermatogenesis to oogenesis at L4/adult molt); Class III = gonads with severely defective DNA morphology at multiple germ cell stages. Arrows in lower image point to nuclei that appear polyploid or otherwise defective; arrowhead indicates what appear to be spermatid nuclei in mid-distal region of gonad. (C) Example of *rbbp-5(tm3463)* gonad exhibiting Emo phenotype; the arrow points to a megaploid oocyte. (D) Summary of types and frequency of each phenotype observed in indicated strains at 25°C. Scale bars = 20 um.
doi:10.1371/journal.pgen.1001349.g009

spermatogenesis to oogenesis in the germline had failed to occur (Figure 9B and 9D; Class II). An additional 19% of sterile *wdr-5.1* mutant animals had germ cells with severely abnormal DNA morphology and many apparently polyploid nuclei. The cells within the gonads of these animals were also disorganized; we observed what appeared to be spermatids in the mid-pachytene zone of some gonads (Figure 9B; Class III). Interestingly, 100% of the *rbbp-5(tm3463)* animals raised at 25°C were Emo and the other phenotypes were not observed (Figure 9C and D).

The Emo phenotype in hermaphrodites can be caused by ovulation defects, which can result from either oocyte defects or defective sperm signaling defects, leading to misregulated re-entry into the cell cycle [74]. To test if the Emo phenotype in *wdr-5.1* and *rbbp-5* mutants was due to defective sperm in these animals, sterile *wdr-5.1* and *rbbp-5* animals grown at elevated temperature were mated with wild type males. We found that fertility could be at least partially rescued by WT sperm, suggesting that sperm defects contribute to the Emo phenotype in these animals (not shown).

Discussion

Our data provide evidence that conserved Set1/MLL components regulate global H3K4 methylation in early embryos. We also show evidence that only a subset of the canonical Set1/MLL components modulates H3K4 methylation in the post-embryonic germline stem cells of *C. elegans*. Assuming that, as in mammals and yeast, these components function in complexes, then there may be multiple complexes that share WDR-5.1 and RBBP-5, with SET-2 providing H3K4me3-specific HMT activity in one or a subset of these. Interestingly, the Set1/MLL-dependent activities do not seem to be completely dependent on ongoing transcription, in contrast to the related COMPASS complex in yeast. Instead a separate, and as yet unidentified mechanism appears to provide

transcription-coupled H3K4 methylation in *C. elegans*. The loss of Set1/MLL activities that require WDR-5 and RBBP-5 is detrimental to normal development, function, and generational maintenance of germ cells in *C. elegans*, illustrating the importance of this core complex in maintaining and regulating the germline cycle as it transits across generations. Furthermore, individual mutants in the different complex homologs exhibit different spectra of somatic and germline phenotypes, indicating that these proteins may also function in unique contexts in different tissues.

H3K4 methylation is regulated by different complexes in different tissues and developmental stages

Set1 is the only identified H3K4 HMT in *S. cerevisiae* and is solely responsible for H3K4 methylation in this organism. The yeast Set1-associated complex (COMPASS) is composed of seven subunits: Swd1-3, Swd2, Swd1, Bre1, Sdc1, Spp1 and Shg1 [12–15]. The Swd1 and Swd3 subunits are considered to be essential for complex stability and hence HMT activity. Sdc1 and Bre2 are required to stimulate transition from di- to trimethylation of H3K4, while Spp1 plays a role in H3K4 trimethylation efficiency [5,25,26].

The organization of the Set1/MLL complexes in metazoans seems to be different from that of COMPASS. There are multiple HMTs with non-redundant functions, and the different HMTs function in the context of slightly different complexes [10,17, 21,75]. Most, if not all, appear to share a common platform composed of WDR5, RbBP5 and ASH2L [10]. This metazoan "core platform" is shared among different Set1/MLL complexes that differentially regulate H3K4 methylation in different tissues or developmental stages [10,75,76].

All of the COMPASS and Set1/MLL components except Shg1 have orthologs in worms. We demonstrated that WDR-5.1, RBBP-5, ASH-2, CFP-1, and DPY-30 are all non-redundantly required for normal, global H3K4me2/3 maintenance in early embryos, strongly indicating that a complex that includes all of these factors is involved, although any individual complex could interact with either SET-2 and/or a different HMT (Figure 1). Interestingly, in the post-embryonic germ line only WDR-5.1/Swd3 and RBBP-5/Swd1 are essential for the normal maintenance of H3K4me2/3 in germline stem cells, while the other components appear to be dispensable.

Strikingly, we observed no significant requirement for ASH-2 for H3K4 methylation in adult germline stem cells, although ASH-2 is required in embryos and is the homolog of Ash2L, an essential member of the core complex in mammalian cells. This is inconsistent with a recent report that concluded that ASH-2 affects lifespan through regulation of H3K4 methylation in germ cells; although a germ cell-specific defect in H3K4me after *ash-2(RNAi)* was not directly shown in that study [77]. Our results suggest that H3K4 methylation activity in the GSCs, if indeed it is operating within a complex, involves a complex with a unique, and potentially novel, subunit composition. Importantly, whereas H3K4me3 levels are nearly undetectable in *set-2, wdr-5.1*, and *rbbp-5* mutant GSCs, H3K4me2 loss was not as complete in the *wdr-5.1* and *rbbp-5* mutants, and unaffected in *set-2* mutants in early embryos and the adult GSCs. It is possible this represents a partial redundancy for a separate WDR5 isoform (e.g., WDR-5.2 and WDR-5.3), a more complex dynamics of the two levels of H3K4 methylation, or a role for another mechanism that is not dependent on WDR5 or RBBP-5.

Interestingly, in both embryos and post-embryonic germ cells, SET-2 is only required for H3K4me3 but not H3K4me2, while two core complex proteins, WDR-5.1 and RBBP-5, affect both modifications. This finding indicates that H3K4me2 and H3K4me3 may require distinct HMTs that rely on the same core complex containing at least WDR-5.1 and RBBP-5. Although we have not done an exhaustive combinatorial deletion/RNAi analysis of all SET protein candidates, it is interesting to note the reports showing that the core MLL complex in other species can exhibit H3K4 HMT activity in the absence of the MLL subunit [38]. H3K4 dimethylation in early embryo and GSC chromatin could involve a complex that includes WDR-5.1 and RBBP-5, but may not include a SET domain protein.

Notably, WDR-5.1/RBBP-5-independent, and presumably transcription-coupled, H3K4 HMT activities are predominant in cells of mid-to-late stage embryos and meiotic germ cells, and at very low levels in early embryos and the GSCs. To attempt to identify the HMT involved, we also tested numerous SET domain candidates by RNAi in the *wdr-5.1(ok1417)* mutant background, but did not observe any significant changes in H3K4 methylation (data not shown). A recent report concluded that SET-16 is an H3K4-specific HMT required for efficient attenuation of Ras signals in some somatic lineages, and reported a decrease in total H3K4me using Western blot analyses [27]. We did not observe significant H3K4me2/3 decreases by immunofluorescence in either early embryos or adult germ cells in *set-16(gk438)* mutants or *set-16(RNAi)*.

Notably, the transcription-dependent process and H3K4me1 levels in chromatin are both largely independent of Set1/MLL components. This could indicate that this activity is only capable of single methyl group transfers, and that the transcription-dependent H3K4me2 and H3K4me3 levels that we observe result from reiterative RNA Pol II initiation events (and subsequent additional methylation) at active loci. It will be interesting to determine what HMTs and/or complexes are responsible for WDR5/RBBP-5-independent H3K4 methylation.

The Set1/MLL activities can operate independently of transcription in *C. elegans*

Yeast Set1 is recruited to chromatin through the RNA polymerase II elongation machinery. As a result, yeast Set1 HMT activity is dependent upon transcription activation, and H3K4 methylation is thus associated with transcribing genes [8,9]. In contrast, our data indicate that Set1/MLL and WDR-5.1/RBBP-5 mediated H3K4 methylation may not strictly rely on active transcription in *C. elegans*. First, H3K4me2/3 is maintained by Set1/MLL components in early germline precursors, cells that have been shown to lack significant levels of active RNA Pol II transcription [58]. The H3K4me we observe in the P cell chromatin (and indeed chromatin in all blastomeres) is densely distributed throughout all chromosomes (an exception being the paternal X [51]), and this distribution seems inconsistent with low levels of active transcription of a small number of genes, or confined to Pol I or Pol III transcription. Second, although zygotic transcription of some genes can be detected in early somatic blastomeres [78], the genome appears to be also largely quiescent in these cells, and bulk zygotic genome activation is not thought to occur until later embryonic stages [59]. Indeed, H3K4 methylation in the early somatic blastomeres is also unaffected by *ama-1* and *cdk-9* RNAi indicating that the bulk of H3K4me is also maintained in a transcription-independent process in these cells. Third, whereas *ama-1* RNAi is able to deplete SET-2/WDR-5.1/RBBP-5 independent H3K4 methylation in meiotic nuclei, the H3K4 methylation in GSCs that depends on these proteins is unaffected by substantial loss of AMA-1 activity. Fourth, the detection of H3K4me in chromatin is not a reliable indicator of productive transcription in *C. elegans* germ line, in which disrupted correlations between RNA Pol II activity, or signs thereof, and

H3K4me regulation are apparent at multiple developmental stages. For example, in the embryonic germline there is a transient appearance of phosphoSer2-modified RNA Pol II in the PGCs, which antithetically coincides with a dramatic genome-wide erasure of H3K4me2 [53].

We cannot rule out that the Set1/MLL components may also be capable of participating in transcription-coupled H3K4 methylation; indeed, there are reduced H3K4me2 and H3K4me3 levels observed in meiotic germ cell chromatin in the *wdr-5.1* and *rbbp-5* mutants. This may indicate either an additional role for these proteins in transcription-dependent accumulation of these marks, or a requirement for WDR-5.1/RBBP-5 dependent marks to achieve normal levels of H3K4 methylation during transcription (or normal transcription itself). Regardless, our evidence suggests these processes can operate independently in germ cells. A summary of the disconnected dynamics between RNA Pol II CTD phosphorylation and H3K4me3 in wild type and *wdr-5.1/rbbp-5* mutants through the germline cycle, summarizing from this study and published work, is illustrated in Figure 10.

In the L1 larva, there is an initial coincidence of active Pol II transcription activation and the WDR-5.1/RBBP-5/SET-2 independent mode of methylation in the expanding population of germ cells. Interestingly, once the GSC population becomes established from the founder PGCs, the mode of H3K4 methylation switches to what appears to be a largely transcription-independent or maintenance mode in the GSCs. A hypothetical reason for this switching of modes could be that the initial reactivation of transcription, and its accompanying transcription-dependent H3K4 methylation, could be used to re-establish, or reinforce, a germ cell-specific "epigenome" that is then maintained in the GSCs by the WDR-5.1/RBBP-5 dependent mechanisms. This could be guided, in part, by other epigenetic marks, such as H3K27 and H3K36 methylation imposed by the *C. elegans* germ-cell enriched, PRC2-related MES-2/3/6 complex and the metazoan-specific H3K36 HMT MES-4, respectively [79]. We have also found that H3K4me2 incorporated during adult germ cell development appears to contribute to the distribution of this mark in both gametes and subsequently in early embryos (J. Arico and W. Kelly, manuscript submitted). The overall pattern inherited by the embryo from the gametes may be maintained in a Set1/MLL component-dependent manner in early cell divisions (this study), thus completing the germline epigenome cycle.

The loss of WDR-5.1 or RBBP-5 leads to defects in germ cells that include a defect in sperm development, which contributes to the Emo phenotype. Mutations in these genes also lead to progressive germ cell defects in later generations (e.g., the observed temperature sensitive mortal germline defect). This indicates that successive passage of the genome through the compromised epigenetic environment of these mutants leads to progressive defects from successive failure, during multiple rounds of the germ cell cycle, to properly maintain the epigenome. The temperature dependence of these phenotypes is not unusual for germline processes; indeed, we have previously described a null mutation in the gene *emb-4* that yields a temperature-sensitive maternal effect embryonic lethality and that also shows defective H3K4 methylation dynamics in the PGCs [80]. Importantly, we cannot rule out the functions for *wdr-5.1* and *rbbp-5* that might be independent of their role in the maintenance of H3K4 methylation, since the H3K4me defects in these mutants were present at both 20°C and 25°C while the phenotypes are far more severe at 25°C. This is an important question that we are currently addressing.

A recent report showed that mutations in *wdr-5.1*, *ash-2*, or *set-2* result in an increase in lifespan in *C. elegans* [77]. In that study it was shown that the enhanced lifespan increase was not observed in animals that lacked GLP-1 function, a Notch receptor required to

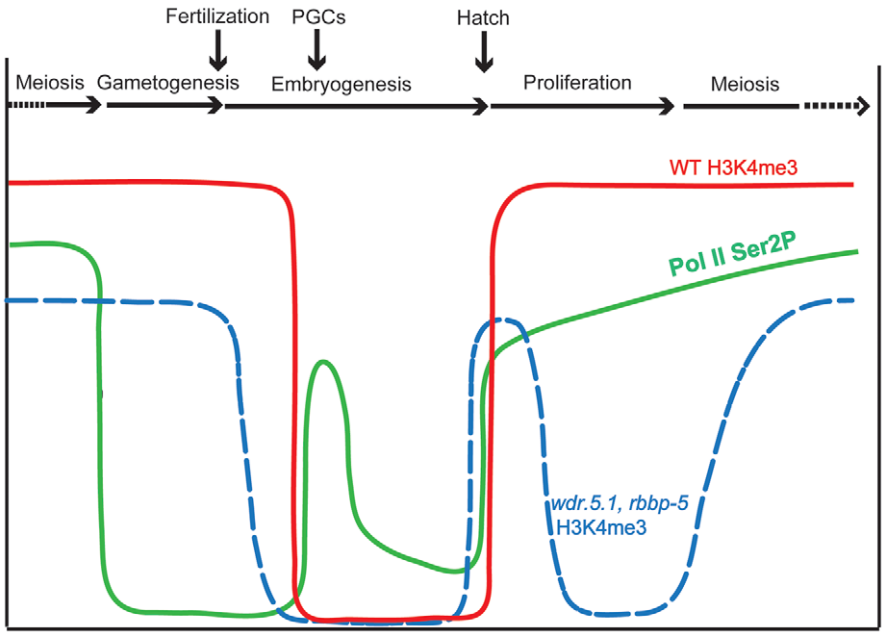

Figure 10. Summary of H3K4me3 and RNA polymerase C-terminal domain phosphorylation dynamics during the *C. elegans* germline cycle. Relative abundance of H3K4me3 in germ cell chromatin at different stages of germ cell development (indicated across the top of the graph) is plotted for wild type (WT; red solid line) and both *wdr-5.1* and *rbbp-5* mutants (blue dotted line). Superimposed on this are the dynamics observed (in WT) for the phosphorylation of Serine 2 of the C-terminal domain repeat of RNA Pol II (pSer2; green line; data from [68]). Notice that pSer2 is absent in the P-cells, in which H3K4me3 is maintained, and that loss of H3K4me3 occurs in the P-cell/PGC stage despite the appearance of pSer2.
doi:10.1371/journal.pgen.1001349.g010

maintain the post-embryonic proliferating germline stem cell population. It was concluded that the germline function of the Set1/MLL complex contributes to its role in lifespan. Our results could imply that it is the GSC-specific role for this complex that may play a more direct role in lifespan. However, we did not observe a role for ASH-2 in either stem cell maintenance or H3K4 methylation in our studies, whereas *ash-2* mutants were observed to have an extended lifespan. This may further indicate that these Set1/MLL components play roles that may not be tied to their function in H3K4 methylation.

It is becoming increasingly clear that epigenetic processes guide germline establishment and the trans-generational maintenance of this totipotent lineage in many, if not all, metazoans. Although there has been much focus on the role of erasure mechanisms during epigenetic reprogramming, there is also a requirement to establish and/or maintain epigenetic information that contributes to pluripotency. This is especially true in the germ line, the lineage that transports both the DNA and its epigenetic content across generations. Any changes or defects in establishment, maintenance, or selective erasure of the epigenetic content required during any stage of the germ cell cycle encounters the strong selective filter of fertility. Our results suggest that this filter may act through alternating cycles of transcription-dependent establishment and transcription-independent maintenance of histone methylation. We propose that these mechanisms help provide and maintain a germline-specific epigenome that contributes to the underlying basis of the totipotency of this lineage.

Materials and Methods

Worm strains

C. elegans strains were maintained using standard conditions at 20°C unless otherwise noted. N2 (Bristol) was used as the wild-type *C. elegans* strain. The following mutant strains were used in this study: *set-2(tm1630)III, wdr-5.1(ok1417)III, wdr-5.2(ok1444)X, rbbp-5(tm3463)II, set-16(gk438)III and eri-1(mg366)IV*. The *wdr-5.1::GFP* transgenic strain was a generous gift from Dr. F. Palladino, Ecole Normale Superieure de lyon, France.

RNAi analysis

Double stranded RNA (dsRNA) corresponding to *set-2, wdr-5.1, rbbp-5, ash-2, dpy-30, cfp-1, wdr-82,* or *ama-1* were generated using the Ribomax Large Scale RNA production kit (Promega). L4 staged *eri-1(mg366)* or WT animals were soaked in 1ug/ul of dsRNA for 24 hours at 20°C. The worms were then transferred to feeding plates containing bacteria expressing dsRNA targeting the corresponding gene, or carrying the empty L4440 vector for control experiments. After the first 24 hours, the worms (P0) were transferred to a new set of feeding plates. The worms (P0) were dissected after 24-48 hours and stained as described below. In some experiments F1 animals and their F2 progeny were also analyzed in immunofluorescence experiments, and/or assessed for embryonic lethality and sterility. For *ama-1*, wild-type or mutant L4 larvae were picked and soaked in either 0.5ug/ul dsRNA in 1x soaking buffer, or buffer alone for 24 hours at 20°C. The worms were then transferred to feeding plates with bacteria expressing the same dsRNA for an additional 24-30 hrs. Worms were dissected, fixed and prepared for immunofluorescence analyses 50 hours post soaking.

Immunofluorescence

Worms were dissected and fixed in paraformaldehyde/methanol [68] for H3K4me2/3, AMA-1, GFP, 8WG16 and SYP-1 staining. A methanol/acetone fixation procedure [81] was used for L1-L4 larvae staining. Samples were fixed in methanol/formaldehyde for H5 staining as described [68]. Rabbit anti-H3K4me3 (1:1000) and anti-H3K4me1 polyclonal antibodies were purchased from Abcam (ab8580 and ab8895, respectively). Mouse monoclonal antibodies against H3K4me3 (CMA 304; 1:1000) and H3K4me2 (CMA303; 1:20) were gifts from Dr. Hiroshi Kimura (Osaka University, Japan [66]). Mouse monoclonal antibody against GFP (MAB3580 1:500), Rabbit polyclonal (07-030 1:1000) and monoclonal (05790 1:1000) antibodies against H3K4me2 were purchased from Millipore. Monoclonal antibody OIC1D4 (1:5) and rabbit anti-PGL (1:10000) were gifts from Dr. S. Strome, UC Santa Cruz. The RNA polymerase II monoclonal antibodies used to detect AMA-1 protein (clone 8WG16 1:100) and phosphoserine 2 isotope of RNA Pol II (clone H5 1:50) were purchased from Covance (MMS-126R and MMS-129R, respectively). Rabbit anti-SYP-1 (1:100) was a gift of Dr. A. Villeneuve, Stanford University. All secondary antibodies were purchased from Molecular Probes and were used at 1:500 dilutions: goat anti-mouse IgG (Alexafluor 488); goat anti-rabbit IgG (Alexafluor 594), donkey anti-rabbit IgG (Alexafluor 488); donkey anti-mouse IgG (Alexafluor 594). DAPI (Sigma, 2 ug/ul) was used to counter-stain DNA. Worms were mounted in anti-fade reagent (Prolong Gold, Molecular Probes). Images were collected using a Leica DMRXA fluorescence microscope and analyzed with Simple PCI software (Hamamatsu Photonics). To quantify the immunofluorescence signals, the mean fluorescence intensity was measured for middle focal plane images of each nucleus from Z-stack images collected for each sample and normalized to the fluorescence signal obtained for DAPI. For all compared samples, the exposure time for each probe was set below image saturation for the brightest nucleus among the samples being compared.

Western blot analysis

Worms were washed from OP50 plates and bleached to collect embryos. To remove egg shells, the embryos were subsequently treated with 1 U/ml chitinase (Sigma, C6137) in egg buffer (25 mM HEPES pH 7.4, 118 mM NaCl, 48 mM KCl, 2 mM $MgSO_4$, 2 mM $CaCl_2$) at 20°C for 40 min, and were boiled in 1X SDS-PAGE sample buffer. The samples were loaded and run on a 15% SDS-PAGE gel and transferred to PVDF membrane. The proteins were probed with the following antibodies: rabbit polyclonal anti-H3 at 1:10,000 (Abcam ab1791), rabbit polyclonal anti-H3K4me3 at 1:3,000 (ab8580), mouse monoclonal anti-H3K4me2 at 1:100 (gift from Dr. Hiroshi Kimura, Osaka University, Japan), rabbit polyclonal anti-H3K4me1 at 1:1000 (ab8895).

Peptide pulldown assays

Biotinylated peptides corresponding to the N-terminus of histone H3 were used for peptide affinity analyses of WDR-5.1 in worm nuclear extracts. Biotinylated H3 (unmodified) and H3 (dimethyl-Lys4) peptides were purchased from Millipore (Cat#12-403 and 12-460, respectively). Biotin conjugated H3 peptides asymmetrically dimethylated at Arg2 (H3R2me2a) were synthesized by the Keck Biotechnology Resource at Yale University. For the binding assay, mixed-stage WT worms were washed off plates with PBS, washed 3X in PBS with protease inhibitor cocktail (Roche), and the worms were frozen at -80°C. To isolate the nuclei, the worm pellet was thawed and ground by mortar and pestle in 2x volume of Nuclear Isolation Buffer (NIB; 25 mM HEPES (pH 7.5), 25 mM KCl, 0.1 mM EDTA, 0.1 mM DTT, 10 mM $MgCl_2$ and 0.5 M sucrose) in liquid nitrogen. The samples were then transferred to a homogenizer in NIB buffer and stroked 20 times on ice. Nuclei were collected by centrifugation. Nuclear

proteins were extracted in Nuclear Extract Buffer (NEB 20 mM HEPES (pH 7.5), 2 mM EDTA, 25% glycerol and 0.1% NP-40) with 350 mM KCl. Prior to pulldown, the nuclear extracts were diluted with NEB buffer without KCl to obtain a solution with 150 mM KCl. The peptide pull down assay was performed according to Wysocka, et al [82]. Briefly, the extracts were incubated with peptides pre-bound to avidin beads overnight at 4°C. After washing with HEPES buffer containing 150 mM KCl for 3 times, the beads were then boiled in 1X SDS buffer and subjected to western blot analysis for WDR-5.1 detection. The WDR-5.1 rabbit antiserum was generated via immunization with a peptide comprising the last 15 C-terminal amino acids of WDR-5.1 (Pickcell Laboratories, The Netherlands). Anti-WDR-5.1 antibodies were affinity purified on Affi-Gel 15 columns (Bio-Rad Laboratories).

Temperature-sensitive (ts) phenotypic analysis

WT and mutant L4 worms (P0) were picked and shifted to 25°C. F1 embryos were counted to score embryonic lethality. To score sterility, 100 L1 larvae of animals grown at 25°C were picked onto separate plates pre-warmed to 25°C. Sterile adult offspring were counted 24 hours post L4 based on an absence of embryos in the uterus. The sterile animals were dissected to extrude gonads, and the whole-mount fixed samples were stained with anti-SYP-1 antibody and counter stained with DAPI. The images were collected on a Leica DMRA microscope. The length of mitotic regions (MR) were measured by counting the number of aligned nuclei from the distal tip of the gonads to the either the appearance of the characteristic crescent-shaped transition zone nuclei and/or the appearance of anti-SYP-1 immunofluorescence. The number of nuclei on one focus plane of DAPI images was used to reflect the length of mitotic zone.

Brood size and mortal germline assay

10 L4 worms were picked and incubate at 20°C or 25°C. F1 embryos were counted for brood size. To score sterility, 100 L1 larvae of F1 from 20°C or 25°C plates were picked onto a new set of plates and kept at the corresponding temperatures. Sterile adult F1 animals were identified and counted based on the lack of embryos *in utero*.

Supporting Information

Figure S1 Knockdown of *set-16* does not affect H3K4me3 in adult germ cells. L4 larvae of *eri-1(mg366)* were soaked in *set-16* dsRNA, or 1x soaking buffer in control samples for 24 hours at 20°C and recovered on feeding plates with bacteria expressing *set-16* dsRNA. F1 animals were continuously exposed to RNAi feeding during subsequent growth. Dissected and whole-mount fixed gonads from F1 adult animals were stained with H3K4me3 antibodies and counter-stained with DAPI. Exposure times were the same for each condition. Bars = 10um. (A, B, E and F) H3K4me3 in the germ cell nuclei of distal region of gonad was not affected by knockdown of *set-16*. Gonads are displayed with the distal regions to the left. (C, D, G and H) H3K4me3 in meiotic germ cells was not significantly decreased in *set-16* RNAi knockdown. (I) Graph of anti-H3K4me3 signal from fluorescence microscopy of adult germ cell nuclei. Quantification was done as in Figure 4. Anti-H3K4me3 signals (arbitrary units ± SEM) were normalized to distal region nuclei from RNAi controls.
Found at: doi:10.1371/journal.pgen.1001349.s001 (1.05 MB TIF)

Figure S2 *wdr-5.1 (ok1417)* is a null mutation. Lysates from mixed stage wild type and *wdr-5.1 (ok1417)* populations were analyzed by Western blot using an affinity-purified anti-WDR-5.1 polyclonal antibody. A band corresponding to the predicted MW of WDR-5.1 was present in wild type but absent in *wdr-5.1 (ok1417)* mutant. This antibody also detects a non-specific band at >80 kDa.
Found at: doi:10.1371/journal.pgen.1001349.s002 (0.80 MB TIF)

Figure S3 Set1/MLL-independent H3K4 methylation is detectable in later stages of embryogenesis. Comma- stage to 1 ½-fold stage embryos from wild-type, *wdr-5.1(ok1417),* and *rbbp-5(tm3463)* animals, or *eri-1(mg366)* animals treated with either control RNAi or *ash-2(RNAi)* were fixed and stained for H3K4me2 or H3K4me3 (as indicated), and counter stained with DAPI. Arrows indicate nuclei with significant levels of H3K4me2/3 despite loss of the indicated Set1/MLL components. Scale bars = 10um.
Found at: doi:10.1371/journal.pgen.1001349.s003 (1.63 MB TIF)

Figure S4 WDR-5.1 interaction with H3 peptides is independent of Lys4 methylation but influenced by Arg2 methylation. Nuclear extracts from WT (N2) were incubated with biotinylated histone H3 N-terminal peptides either unmodified on K4 (H3K4me0), dimethylated on K4 (H3K4me2), or unmodified on K4 and asymmetrically dimethylated on R2 (H3R2me2a). The peptides were incubated with avidin beads, washed, and bound proteins eluted with SDS sample buffer and analyzed by Western blot using anti-WDR-5.1 antibody as probe. Total lysate (5% input) was included as control to identify WDR-5.1. WDR-5.1 was detectably bound to the H3K4me0 and H3K4me2 peptides, but no interaction with H3R2me2a was observed. A control in which no peptide was added to the lysate prior to avidin bead affinity purification is also shown (Avidin lane).
Found at: doi:10.1371/journal.pgen.1001349.s004 (0.21 MB TIF)

Figure S5 *ama-1(RNAi)* depletion of Pol II phospho-Ser2 in embryos. RNAi experiments targeting *ama-1* were done as in Figure 3. The embryos were fixed and stained with either monoclonal antibody (mAb) H5 for the Pol II CTD phospho-Ser2 epitope, or mouse monoclonal antibodies against H3K4me3 as indicated. Exposure times were the same for each antibody for comparison. Bars = 10um. (A) RNAi of *ama-1* depletes the mAb H5 signal to background levels in both WT and *wdr-5.1*. (B) H3K4me3 dependent on *wdr-5.1* is not significantly affected by loss of *ama-1*/phospho-Ser2. (C) RNAi of *cdk-9* also depletes the mAb H5 signal to undetectable levels in WT and H3K4me3 is also not significantly affected.
Found at: doi:10.1371/journal.pgen.1001349.s005 (1.99 MB TIF)

Figure S6 H3K4me3 and H3K4me2 are decreased in *wdr-5.1 (ok1417)* male GSCs. Experiments were performed as in Figure 4. (A) H3K4me3 is depleted from the distal region of gonad in *wdr-5.1(ok1417)* mutant males. (B) H3K4me2 is substantially reduced in *wdr-5.1(ok1417)* male germ cells. Bar = 20um.
Found at: doi:10.1371/journal.pgen.1001349.s006 (1.03 MB TIF)

Figure S7 Schematic of RNAi protocol used to target Set1/MLL component homologs.
Found at: doi:10.1371/journal.pgen.1001349.s007 (0.63 MB TIF)

Figure S8 H3K4me3 levels are reduced in all adult germ cell stages in *wdr-5.1* mutant gonads. Dissected and whole-mount fixed gonads from wild-type (A, A') and *wdr-5.1(ok1417)* (B, B') adult hermaphrodites were probed with antibodies to H3K4me3 (A' and B') and counterstained with DAPI (A and B). Gonad arms are displayed with the distal regions to the left. Images were taken with identical exposure time for comparison. As in Figure 4, H3K4me3 is most strongly depleted from the chromatin of the distal region germ cells; however, significant decreases were also observed in more proximal pachytene and diakinesis regions. Bars = 10 um.

(C) Quantification of anti-H3K4me3 IF signal in individual pachytene and diakinetic nuclei of wild-type and *wdr-5.1(ok1417)* nuclei. Mean IF signal of anti-H3K4me3 signal in single nuclei were measured and analyzed as in Figure 4. 20 pachytene nuclei from 4 gonads (5 nuclei/gonad) were measured and analyzed, and, 12 diakinetic oocyte nuclei from 4 gonads (3 nuclei/gonad) were measured and analyzed. Signals were compared to those from wild type nuclei which were arbitrarily set to 1. Error bars = SEM.
Found at: doi:10.1371/journal.pgen.1001349.s008 (1.33 MB TIF)

Figure S9 H3K4me2 levels are reduced in all adult germ cell stages in *wdr-5.1* mutant gonads. The gonads of wild type and *wdr-5.1 (ok1417)* were probed with a mouse monoclonal antibody specific for H3K4me2 (mAb CMA303). The experiment was performed as in Figure 5. Images in (A) and (B) were taken with identical exposure time for each probe (except in C) and at the same magnification for comparison. (A) H3K4me2 was present in all the nuclei of gonad in wild type. (B) H3K4me2 was significantly decreased, but not totally depleted in *wdr-5.1 (ok1417)* mutant. (C) Prolonged exposure of *wdr-5.1* GSC H3K4me2 immunofluorescence. The low level of WDR-5.1-independent H3K4me2 in the GSCs exhibits a striking speckled pattern on the chromatin when observed with longer exposure times than that of the wild type image shown. Bars = 10 um. (D) Quantification of anti-H3K4me2 IF signal in individual pachytene and diakinetic nuclei of wild-type and *wdr-5.1(ok1417)* nuclei. Data was collected and analyzed as in Figure S8. For quantification in pachytene, 20 nuclei from 4 gonads (5 nuclei/gonad) were measured and analyzed. For qualification of diakinetic nuclei, 12 nuclei from 4 gonads (3 nuclei/gonad) were measured and analyzed. Signals were compared to those in wild type nuclei, which were arbitrarily set to 1. Error bars = SEM.
Found at: doi:10.1371/journal.pgen.1001349.s009 (1.68 MB TIF)

Figure S10 *ama-1(RNAi)* depletion of Pol II phospho-Ser2 in adult germ cells. RNAi experiments were done as in Figure 6. Adult hermaphrodite gonads were dissected and fixed and probed with either mAb H5 for phosphor-Ser2 or mouse monoclonal antibodies against H3K4me3 as indicated. Exposure times were the same for each antibody for comparison. Bars = 10um. (A and B) RNAi of *ama-1* depletes the mAb H5 signal to background levels in both WT and *wdr-5.1* adult germ cells. (C and D) Similar H3K4me3 patterns as described for Figure 6 were observed.
Found at: doi:10.1371/journal.pgen.1001349.s010 (1.12 MB TIF)

Figure S11 Temperature-dependent fertility and germline mortality defects in *wdr-5.1(ok1417)* mutants. (A) 10 WT or *wdr-5.1(ok1417)* hermaphrodites were grown continuously at 20°C, or were shifted to 25°C as L4 larvae and their F1 progeny were counted. (B) *wdr-5.1(ok1417)* L4 larvae were shifted to 25°C, and 100 F1 larvae were picked onto separate plates and scored for sterility. Fertile animals at each subsequent generation were further maintained at 25°C and the sterility of their offspring (F2-F6) was assessed.
Found at: doi:10.1371/journal.pgen.1001349.s011 (0.33 MB TIF)

Figure S12 Egl and Dpy phenotypes in *wdr-5.1(ok1417)* and *rbbp-5(tm3463)* mutants. (A) DIC images of *wdr-5.1(ok1417)* and *rbbp-5(tm3463)* adults compared to wild type illustrating Egl defect; i.e., extensive accumulation of embryos *in utero*. Arrows mark late staged embryos not normally observed in wild type uteri. (B) *rbbp-5(tm3463)* and wild type adult animals at same magnification, illustrating the Dpy phenotype observed in the *tm3463* strain.
Found at: doi:10.1371/journal.pgen.1001349.s012 (1.64 MB TIF)

Acknowledgments

We wish to acknowledge the Caenorhabditis Genetics Center (CGC, Minneapolis, MN, USA) for providing *C. elegans* strains used in this work and members of the Kelly lab and Emory Chromatin Interest Group for helpful discussions and critical review of the manuscript. We also wish to thank the anonymous reviewers for their helpful critiques during the submission of this manuscript.

Author Contributions

Conceived and designed the experiments: TL WGK. Performed the experiments: TL. Analyzed the data: TL WGK. Wrote the paper: TL WGK.

References

1. Li B, Carey M, Workman JL (2007) The role of chromatin during transcription. Cell 128: 707–719.
2. Fischle W, Wang Y, Allis CD (2003) Histone and chromatin cross-talk. Curr Opin Cell Biol 15: 172–183.
3. Sims RJ, 3rd, Reinberg D (2006) Histone H3 Lys 4 methylation: caught in a bind? Genes Dev 20: 2779–2786.
4. Dillon SC, Zhang X, Trievel RC, Cheng X (2005) The SET-domain protein superfamily: protein lysine methyltransferases. Genome Biol 6: 227.
5. Ng HH, Robert F, Young RA, Struhl K (2003) Targeted recruitment of Set1 histone methylase by elongating Pol II provides a localized mark and memory of recent transcriptional activity. Mol Cell 11: 709–719.
6. Krogan NJ, Dover J, Wood A, Schneider J, Heidt J, et al. (2003) The Paf1 complex is required for histone H3 methylation by COMPASS and Dot1p: linking transcriptional elongation to histone methylation. Mol Cell 11: 721–729.
7. Pokholok DK, Harbison CT, Levine S, Cole M, Hannett NM, et al. (2005) Genome-wide map of nucleosome acetylation and methylation in yeast. Cell 122: 517–527.
8. Santos-Rosa H, Schneider R, Bannister AJ, Sherriff J, Bernstein BE, et al. (2002) Active genes are tri-methylated at K4 of histone H3. Nature 419: 407–411.
9. Briggs SD, Bryk M, Strahl BD, Cheung WL, Davie JK, et al. (2001) Histone H3 lysine 4 methylation is mediated by Set1 and required for cell growth and rDNA silencing in Saccharomyces cerevisiae. Genes Dev 15: 3286–3295.
10. Dou Y, Milne TA, Ruthenburg AJ, Lee S, Lee JW, et al. (2006) Regulation of MLL1 H3K4 methyltransferase activity by its core components. Nat Struct Mol Biol 13: 713–719.
11. Krogan NJ, Dover J, Khorrami S, Greenblatt JF, Schneider J, et al. (2002) COMPASS, a histone H3 (Lysine 4) methyltransferase required for telomeric silencing of gene expression. J Biol Chem 277: 10753–10755.
12. Shilatifard A (2006) Chromatin modifications by methylation and ubiquitination: implications in the regulation of gene expression. Annu Rev Biochem 75: 243–269.
13. Nagy PL, Griesenbeck J, Kornberg RD, Cleary ML (2002) A trithorax-group complex purified from Saccharomyces cerevisiae is required for methylation of histone H3. Proc Natl Acad Sci U S A 99: 90–94.
14. Roguev A, Schaft D, Shevchenko A, Aasland R, Shevchenko A, et al. (2003) High conservation of the Set1/Rad6 axis of histone 3 lysine 4 methylation in budding and fission yeasts. J Biol Chem 278: 8487–8493.
15. Dehe PM, Geli V (2006) The multiple faces of Set1. Biochem Cell Biol 84: 536–548.
16. Miller T, Krogan NJ, Dover J, Erdjument-Bromage H, Tempst P, et al. (2001) COMPASS: a complex of proteins associated with a trithorax-related SET domain protein. Proc Natl Acad Sci U S A 98: 12902–12907.
17. Dou Y, Milne TA, Tackett AJ, Smith ER, Fukuda A, et al. (2005) Physical association and coordinate function of the H3 K4 methyltransferase MLL1 and the H4 K16 acetyltransferase MOF. Cell 121: 873–885.
18. Wysocka J, Swigut T, Milne TA, Dou Y, Zhang X, et al. (2005) WDR5 associates with histone H3 methylated at K4 and is essential for H3 K4 methylation and vertebrate development. Cell 121: 859–872.
19. Milne TA, Dou Y, Martin ME, Brock HW, Roeder RG, et al. (2005) MLL associates specifically with a subset of transcriptionally active target genes. Proc Natl Acad Sci U S A 102: 14765–14770.
20. Wysocka J, Myers MP, Laherty CD, Eisenman RN, Herr W (2003) Human Sin3 deacetylase and trithorax-related Set1/Ash2 histone H3-K4 methyltransferase are tethered together selectively by the cell-proliferation factor HCF-1. Genes Dev 17: 896–911.
21. Hughes CM, Rozenblatt-Rosen O, Milne TA, Copeland TD, Levine SS, et al. (2004) Menin associates with a trithorax family histone methyltransferase complex and with the hoxc8 locus. Mol Cell 13: 587–597.
22. Yokoyama A, Wang Z, Wysocka J, Sanyal M, Aufiero DJ, et al. (2004) Leukemia proto-oncoprotein MLL forms a SET1-like histone methyltransferase complex with menin to regulate Hox gene expression. Mol Cell Biol 24: 5639–5649.

23. Glaser S, Schaft J, Lubitz S, Vintersten K, van der Hoeven F, et al. (2006) Multiple epigenetic maintenance factors implicated by the loss of Mll2 in mouse development. Development 133: 1423–1432.
24. Lee JH, Skalnik DG (2005) CpG-binding protein (CXXC finger protein 1) is a component of the mammalian Set1 histone H3-Lys4 methyltransferase complex, the analogue of the yeast Set1/COMPASS complex. J Biol Chem 280: 41725–41731.
25. Schneider J, Wood A, Lee JS, Schuster R, Dueker J, et al. (2005) Molecular regulation of histone H3 trimethylation by COMPASS and the regulation of gene expression. Mol Cell 19: 849–856.
26. Steward MM, Lee JS, O'Donovan A, Wyatt M, Bernstein BE, et al. (2006) Molecular regulation of H3K4 trimethylation by ASH2L, a shared subunit of MLL complexes. Nat Struct Mol Biol 13: 852–854.
27. Fisher K, Southall SM, Wilson JR, Poulin GB (2010) Methylation and demethylation activities of a C. elegans MLL-like complex attenuate RAS signalling. Dev Biol 341: 142–153.
28. Simonet T, Dulermo R, Schott S, Palladino F (2007) Antagonistic functions of SET-2/SET1 and HPL/HP1 proteins in C. elegans development. Dev Biol.
29. Ruthenburg AJ, Wang W, Graybosch DM, Li H, Allis CD, et al. (2006) Histone H3 recognition and presentation by the WDR5 module of the MLL1 complex. Nat Struct Mol Biol 13: 704–712.
30. Schuetz A, Allali-Hassani A, Martin F, Loppnau P, Vedadi M, et al. (2006) Structural basis for molecular recognition and presentation of histone H3 by WDR5. Embo J 25: 4245–4252.
31. Couture JF, Collazo E, Trievel RC (2006) Molecular recognition of histone H3 by the WD40 protein WDR5. Nat Struct Mol Biol 13: 698–703.
32. Han Z, Guo L, Wang H, Shen Y, Deng XW, et al. (2006) Structural basis for the specific recognition of methylated histone H3 lysine 4 by the WD-40 protein WDR5. Mol Cell 22: 137–144.
33. Kirmizis A, Santos-Rosa H, Penkett CJ, Singer MA, Vermeulen M, et al. (2007) Arginine methylation at histone H3R2 controls deposition of H3K4 trimethylation. Nature 449: 928–932.
34. Guccione E, Bassi C, Casadio F, Martinato F, Cesaroni M, et al. (2007) Methylation of histone H3R2 by PRMT6 and H3K4 by an MLL complex are mutually exclusive. Nature 449: 933–937.
35. Hyllus D, Stein C, Schnabel K, Schiltz E, Imhof A, et al. (2007) PRMT6-mediated methylation of R2 in histone H3 antagonizes H3 K4 trimethylation. Genes Dev 21: 3369–3380.
36. Cosgrove MS, Patel A (2010) Mixed lineage leukemia: a structure-function perspective of the MLL1 protein. Febs J 277: 1832–1842.
37. Patel A, Dharmarajan V, Cosgrove MS (2008) Structure of WDR5 bound to mixed lineage leukemia protein-1 peptide. J Biol Chem 283: 32158–32161.
38. Patel A, Dharmarajan V, Vought VE, Cosgrove MS (2009) On the mechanism of multiple lysine methylation by the human mixed lineage leukemia protein-1 (MLL1) core complex. J Biol Chem 284: 24242–24256.
39. Patel A, Vought VE, Dharmarajan V, Cosgrove MS (2008) A conserved arginine-containing motif crucial for the assembly and enzymatic activity of the mixed lineage leukemia protein-1 core complex. J Biol Chem 283: 32162–32175.
40. Song JJ, Kingston RE (2008) WDR5 interacts with mixed lineage leukemia (MLL) protein via the histone H3-binding pocket. J Biol Chem 283: 35258–35264.
41. Cho YW, Hong T, Hong S, Guo H, Yu H, et al. (2007) PTIP associates with MLL3- and MLL4-containing histone H3 lysine 4 methyltransferase complex. J Biol Chem 282: 20395–20406.
42. Muramoto T, Muller I, Thomas G, Melvin A, Chubb JR (2010) Methylation of H3K4 Is required for inheritance of active transcriptional states. Curr Biol 20: 397–406.
43. Ringrose L, Paro R (2004) Epigenetic regulation of cellular memory by the Polycomb and Trithorax group proteins. Annu Rev Genet 38: 413–443.
44. Petruk S, Sedkov Y, Smith S, Tillib S, Kraevski V, et al. (2001) Trithorax and dCBP acting in a complex to maintain expression of a homeotic gene. Science 294: 1331–1334.
45. Katz DJ, Edwards TM, Reinke V, Kelly WG (2009) A C. elegans LSD1 demethylase contributes to germline immortality by reprogramming epigenetic memory. Cell 137: 308–320.
46. Rechtsteiner A, Ercan S, Takasaki T, Phippen TM, Egelhofer TA, et al. (2010) The histone H3K36 methyltransferase MES-4 acts epigenetically to transmit the memory of germline gene expression to progeny. PLoS Genet 6: e1001091. doi:10.1371/journal.pgen.1001091.
47. Hammoud SS, Nix DA, Zhang H, Purwar J, Carrell DT, et al. (2009) Distinctive chromatin in human sperm packages genes for embryo development. Nature 460: 473–478.
48. Bernstein BE, Mikkelsen TS, Xie X, Kamal M, Huebert DJ, et al. (2006) A bivalent chromatin structure marks key developmental genes in embryonic stem cells. Cell 125: 315–326.
49. Brykczynska U, Hisano M, Erkek S, Ramos L, Oakeley EJ, et al. (2010) Repressive and active histone methylation mark distinct promoters in human and mouse spermatozoa. Nat Struct Mol Biol 17: 679–687.
50. Azuara V, Perry P, Sauer S, Spivakov M, Jorgensen HF, et al. (2006) Chromatin signatures of pluripotent cell lines. Nat Cell Biol 8: 532–538.
51. Bean CJ, Schaner CE, Kelly WG (2004) Meiotic pairing and imprinted X chromatin assembly in Caenorhabditis elegans. Nat Genet 36: 100–105.
52. Seki Y, Yamaji M, Yabuta Y, Sano M, Shigeta M, et al. (2007) Cellular dynamics associated with the genome-wide epigenetic reprogramming in migrating primordial germ cells in mice. Development 134: 2627–2638.
53. Hajkova P, Ancelin K, Waldmann T, Lacoste N, Lange UC, et al. (2008) Chromatin dynamics during epigenetic reprogramming in the mouse germ line. Nature 452: 877–881.
54. Schaner C, Deshpande G, Schedl P, Kelly W (2003) A conserved chromatin architecture marks and maintains the restricted germ cell lineage in worms and flies. Dev Cell 5: 747–757.
55. Vastenhouw NL, Zhang Y, Woods IG, Imam F, Regev A, et al. (2010) Chromatin signature of embryonic pluripotency is established during genome activation. Nature 464: 922–926.
56. Thomson JP, Skene PJ, Selfridge J, Clouaire T, Guy J, et al. CpG islands influence chromatin structure via the CpG-binding protein Cfp1. Nature 464: 1082–1086.
57. Edgar LG, Wolf N, Wood WB (1994) Early transcription in Caenorhabditis elegans embryos. Development 120: 443–451.
58. Seydoux G, Dunn MA (1997) Transcriptionally repressed germ cells lack a subpopulation of phosphorylated RNA polymerase II in early embryos of Caenorhabditis elegans and Drosophila melanogaster. Development 124: 2191–2201.
59. Baugh LR, Hill AA, Slonim DK, Brown EL, Hunter CP (2003) Composition and dynamics of the Caenorhabditis elegans early embryonic transcriptome. Development 130: 889–900.
60. Bernstein BE, Kamal M, Lindblad-Toh K, Bekiranov S, Bailey DK, et al. (2005) Genomic maps and comparative analysis of histone modifications in human and mouse. Cell 120: 169–181.
61. Schneider R, Bannister AJ, Myers FA, Thorne AW, Crane-Robinson C, et al. (2004) Histone H3 lysine 4 methylation patterns in higher eukaryotic genes. Nat Cell Biol 6: 73–77.
62. Martin C, Zhang Y (2007) Mechanisms of epigenetic inheritance. Curr Opin Cell Biol 19: 266–272.
63. Allegrucci C, Thurston A, Lucas E, Young L (2005) Epigenetics and the germline. Reproduction 129: 137–149.
64. Schaner C, Kelly W (2006) Germline Chromatin. Wormbook, ed. The *Celegnas* Research Community. pp 1–14.
65. Starck J, Brun J (1977) Autoradiographic localization of RNA synthesis in vitro during oogenesis in Parascaris equorum. C R Acad Sci Hebd Seances Acad Sci D 284: 1341–1344.
66. Kimura H, Hayashi-Takanaka Y, Goto Y, Takizawa N, Nozaki N (2008) The organization of histone H3 modifications as revealed by a panel of specific monoclonal antibodies. Cell Struct Funct 33: 61–73.
67. Kelly WG, Schaner CE, Dernburg AF, Lee MH, Kim SK, et al. (2002) X-chromosome silencing in the germline of C. elegans. Development 129: 479–492.
68. Furuhashi H, Takasaki T, Rechtsteiner A, Li T, Kimura H, et al. (2010) Trans-generational epigenetic regulation of C. elegans primordial germ cells. Epigenetics Chromatin 3: 1–21.
69. Crittenden SL, Bernstein DS, Bachorik JL, Thompson BE, Gallegos M, et al. (2002) A conserved RNA-binding protein controls germline stem cells in Caenorhabditis elegans. Nature 417: 660–663.
70. Lamont LB, Crittenden SL, Bernstein D, Wickens M, Kimble J (2004) FBF-1 and FBF-2 regulate the size of the mitotic region in the C. elegans germline. Dev Cell 7: 697–707.
71. Austin J, Kimble J (1987) glp-1 is required in the germ line for regulation of the decision between mitosis and meiosis in C. elegans. Cell 51: 589–599.
72. MacQueen AJ, Colaiacovo MP, McDonald K, Villeneuve AM (2002) Synapsis-dependent and -independent mechanisms stabilize homolog pairing during meiotic prophase in C. elegans. Genes Dev 16: 2428–2442.
73. Byrd KN, Shearn A (2003) ASH1, a Drosophila trithorax group protein, is required for methylation of lysine 4 residues on histone H3. Proc Natl Acad Sci U S A 100: 11535–11540.
74. Harris JE, Govindan JA, Yamamoto I, Schwartz J, Kaverina I, et al. (2006) Major sperm protein signaling promotes oocyte microtubule reorganization prior to fertilization in Caenorhabditis elegans. Dev Biol 299: 105–121.
75. Crawford BD, Hess JL (2006) MLL core components give the green light to histone methylation. ACS Chem Biol 1: 495–498.
76. Ruthenburg AJ, Allis CD, Wysocka J (2007) Methylation of lysine 4 on histone H3: intricacy of writing and reading a single epigenetic mark. Mol Cell 25: 15–30.
77. Greer EL, Maures TJ, Hauswirth AG, Green EM, Leeman DS, et al. (2010) Members of the H3K4 trimethylation complex regulate lifespan in a germline-dependent manner in C. elegans. Nature 466: 383–387.
78. Seydoux G, Fire A (1994) Soma-germline asymmetry in the distributions of embryonic RNAs in Caenorhabditis elegans. Development 120: 2823–2834.
79. Bender LB, Suh J, Carroll CR, Fong Y, Fingerman IM, et al. (2006) MES-4: an autosome-associated histone methyltransferase that participates in silencing the X chromosomes in the C. elegans germ line. Development 133: 3907–3917.
80. Checchi PM, Kelly WG (2006) emb-4 is a conserved gene required for efficient germline-specific chromatin remodeling during Caenorhabditis elegans embryogenesis. Genetics 174: 1895–1906.
81. Strome S, Wood WB (1983) Generation of asymmetry and segregation of germline granules in early C. elegans embryos. Cell 35: 15–25.
82. Wysocka J (2006) Identifying novel proteins recognizing histone modifications using peptide pull-down assay. Methods 40: 339–343.